

Self-assembling and self-limiting monolayer deposition

Rüdiger Foest^{1,a}, Martin Schmidt¹, and Hassan Gargouri²

¹ Leibniz Institute for Plasma Science and Technology, Felix-Hausdorff-Str. 2, 17489 Greifswald, Germany

² Sentech Instruments GmbH, Schwarzschildstraße 2, 12489 Berlin, Germany

Received 16 July 2013 / Received in final form 18 November 2013

Published online 4 February 2014 – © EDP Sciences, Società Italiana di Fisica, Springer-Verlag 2014

Abstract. Effects of spatial ordering of molecules on surfaces are commonly utilized to deposit ultra-thin films with a thickness of a few nm. In this review paper, several methods are discussed, that are distinguished from other thin film deposition processes by exactly these effects that lead to self-assembling and self-limiting layer growth and eventually to coatings with unique and fascinating properties and applications in micro-electronics, optics, chemistry, or biology. Traditional methods for the formation of self-assembled films of ordered organic molecules, such as the Langmuir-Blodgett technique along with thermal atomic layer deposition (ALD) of inorganic molecules are evaluated. The overview is complemented by more recent developments for the deposition of organic or hybrid films by molecular layer deposition. Particular attention is given to plasma assisted techniques, either as a preparative, supplementary step or as inherent part of the deposition as in plasma enhanced ALD or plasma assisted, repeated grafting deposition. The different methods are compared and their film formation mechanisms along with their advantages are presented from the perspective of a plasma scientist. The paper contains lists of established film compounds and a collection of the relevant literature is provided for further reading.

1 Introduction

Thin films have a broad field of applications. On the one hand they constitute the frontier between bulk material and environment as they protect the material, e.g., from abrasion or corrosion, or serve as decorative coating. On the other hand they maintain specific functions between two materials (e.g. promote adhesion and release, provide the lubricant, or generate biocompatibility to name a few). In other cases, their benefit can be related to the film itself, such as films in semiconductor devices, solar cells, or thin film optics like optical filters. The thickness of these layers varies from a fraction of nm for monolayers up to some micrometers achieved by repeated process cycles. Thin films can be deposited on a vast variety of substrates; the spectrum of film materials covers very different material classes, from solids to soft matter. The chemistry of thin film material covers both worlds, the inorganic and the organic. Well-established substances include pure metals, inorganic compounds like oxides, nitrides, sulphides, halides or organic compounds. The latter are deposited as layers of organic molecules, as crosslinked polymers with tuneable functionalities [1], and also as metal-organic composite layers. Biocompatible ultra-thin films on implants are advantageous because the introduction of foreign substances into the body is minimized [2]. Furthermore, thin films constitute valuable accessories for studying the in-

teraction of single atoms and molecules with surfaces as well as with each other on surfaces.

Multitude techniques for the deposition of thin films have been developed in the past [3]. Chemical solution deposition transfers the coating solution onto substrates by spin-, dip-, and spray-coating. Chemical electric (electrolytic) procedures operating in liquids are common. Next to these, gas phase procedures which often require vacuum environment are widespread. Classic examples comprise pulsed laser deposition, sputtering and molecular beam epitaxial procedures or evaporation methods. For instance, chemical vapour deposition (CVD) is described by dissociation and chemical reaction of gaseous reactants in an activated environment, followed by heterogeneous chemical reactions at the surface leading to formation of solid films on the substrate. The gaseous raw material is activated by thermal energy or photons. Activation by plasmas leads to plasma assisted or enhanced chemical vapour deposition (PE-CVD). An essential advantage of PE-CVD with respect to CVD is the lower substrate temperature and hence the minimized thermal stress of the substrate. CVD allows the formation of various thin films differentiated by their chemical composition, resulting in diverse chemical, mechanical, optical and electrical properties.

Several experimental methods are successfully applied for investigation of thin films and surfaces concerning, e.g., chemical composition, morphology, thickness, crystal structure and mechanical, chemical, optical, and electrical

^a e-mail: foest@inp-greifswald.de

properties. Scattering techniques are used applying beams of electrons (Auger Electron Spectroscopy), electromagnetic radiation (X-ray Photo-electron Spectroscopy) and ions (Secondary Ion Mass Spectrometry) and detecting the response after the interaction with the sample [4]. Microscopic methods may include scattering effects as Transmission Electron Microscopy, or using other effects by Scanning Probe Microscopy [5] as Scanning Tunneling Microscopy or Atomic Force Microscopy. Reviews concerning surface investigations of self-assembled monolayers in particular Langmuir-Blodgett films [6] and self-assembled organic monolayers [7,8] have been published recently.

The demand for coatings with a high degree of conformity arose particularly from the development of electronic devices to higher integration degree with decreasing linear dimensions. Here, 3-D structures, especially trenches with high aspect ratio, have to be coated with the requirement of equal film thickness on the side wall (1:1 conformity).

The aim of this paper is to give a survey on the deposition of ultra-thin films, with particular consideration of films with excellent conformity even in structures with high aspect ratio. Bottom-up methods are discussed for the formation of self-assembled monolayers (SAM) of organic molecules using self-assembly techniques such as the Langmuir-Blodgett technique [9,10]. Inorganic film formation by atomic layer deposition (ALD) and enhanced by plasma (Plasma ALD, PE-ALD) is reported [11]. Closely related to ALD, molecular layer deposition (MLD) allows the formation of organic and inorganic-organic hybrid films [12]. Surface coating by plasma enhanced repeated grafting deposition (PE-RGD) enables the formation of ultra-thin organic plasma polymers [2]. The role of plasmas is diverse: while several methods rely on plasmas as an inherent part of the process (e.g. PE-ALD, PE-RGD), in other cases additional plasma steps are included merely as preparative step for a subsequent film modification.

Principles of the above deposition methods are presented, their advantages and disadvantages as well as typical applications are discussed.

2 Films of ordered molecules

The preparation of monomolecular organic thin films with a high degree of order and orientation on solid substrates using self-assembly mechanisms can be performed in liquids, in the gas phase or on the liquid-gas interface. The latter is applied for formation of Langmuir-Blodgett films.

2.1 SAM

2.1.1 Formation on liquid-air interface (Langmuir-Blodgett films)

By the Langmuir-Blodgett (LB) technique mono- or multilayers also multilayered hetero-structures are transferred from a liquid-gas interface onto a plane solid substrate [13–17]. This technique mostly uses water as liquid. Langmuir-Blodgett molecules are amphiphilic, i.e.

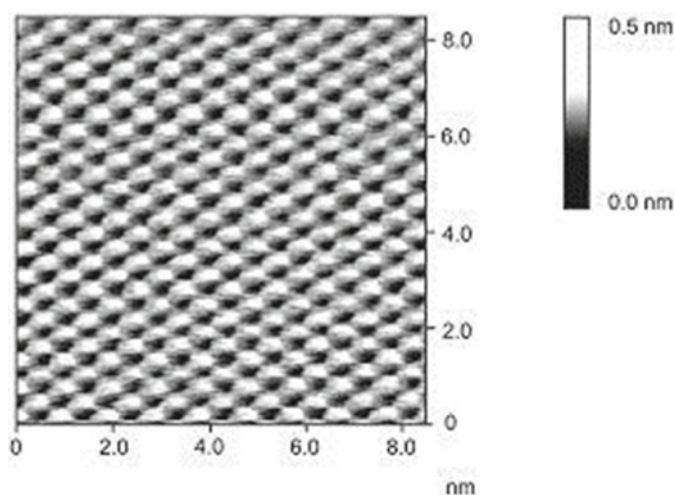


Fig. 1. Surface of a prototypical Langmuir-Blodgett film (12-layer arachidic acid, atomic force micrograph). Reprinted with permission from reference [18] (© 1996, American Chemical Society).

distinguished by hydrophilic and hydrophobic groups that are spatially separated. Examples of organic compounds used for LB films are fatty acids, derivatives of porphyrins, phthalocyanines, and diacetylenes [16]. A representative film is shown in Figure 1. The material is spreading on a water surface with only the hydrophilic group establishing contact to the water (subphase). If the arrangement of molecules is compressed e.g. in a trough by a movable barrier as shown in Figure 2, a so called Langmuir film is formed at the liquid-to-air-interface.

During the movement of the barrier the surface tension increases (Surface tension isotherm). The molecular arrangement with comparably large separation between the molecules is referred to as “gas” phase. Accordingly, the re-organization initiating after the compression of the Langmuir film by the barrier movement has started is comparable to a “liquid” phase with smaller molecule separation length and commencing, yet marginal alignment. The final state with higher surface pressure and tight packaging of aligned molecules is denoted “solid” state on account of the apparent long-range order (Fig. 3, [16]).

The film is transferred to a solid target by slowly moving of the substrate across the air-water interface (Fig. 4). Beside water, other liquids, e.g., mercury, glycerol are custom as subphase [16]. A hydrophilic substrate had to be moved out of the liquid to ensure the contact of the hydrophilic groups of the Langmuir film with the substrate surface. Inversely, a hydrophobic substrate must be immersed into the liquid, so that the hydrophobic ends of the molecules make contact with the substrate surface. Typical substrate materials involve silicon wafers, glass and quartz, or oxidized aluminium, chromium, and tin. Multilayers can be formed by multiple back and forth movement. LB films are generated in the thickness range from ultra-thin in the order of 1 nm up to films of 1 μm with a thickness precision of 1% over large areas and low defect density. Drawbacks are the mechanical softness, the

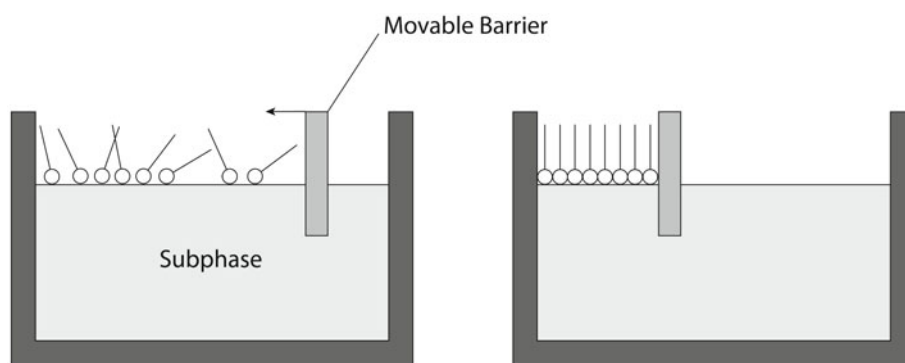


Fig. 2. Formation of Langmuir film on a liquid phase (left: beginning of compression, right: aligned molecules). Reprinted with permission from reference [16] (© IOP Publishing Ltd, 2001).

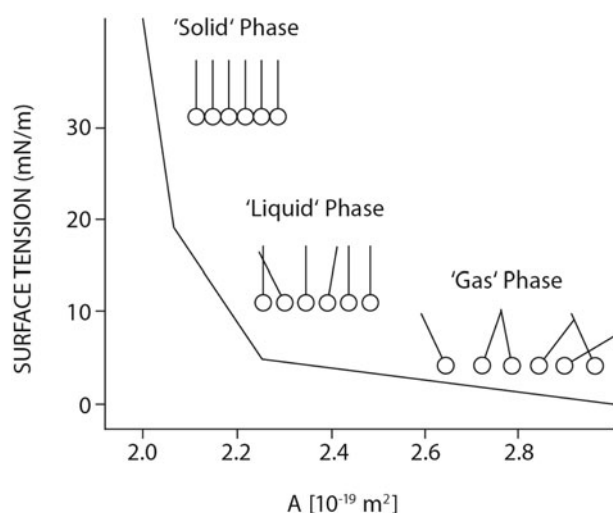


Fig. 3. Schematic tension–area isotherm (surface tension over area per molecule). With pressure increasing, the molecules traverse phases that are denoted in analogy to phase transitions from gaseous via liquid to solid. (Representative example for fatty acid.) Reprinted with permission from reference [16] (© IOP Publishing Ltd, 2001).

limited temperature stability of the films, and the low deposition rate [19].

According to the multitude of customary chemical compounds for the formation of LB films a broad spectrum of applications is studied in the fields of e.g. molecular electronics (organic conductors, magnets, rectifiers) and optics (non-linear optics) [17,20], permeable membranes and lubrication [13] or gas sensor techniques [21]. A subsequent plasma treatment of LB films to enhance their resistance against thermal, chemical or mechanical strain is reported [22–24].

2.1.2 SAM formation on liquid-solid and vapor-solid interface

The ability for spontaneous formation of molecular blocks of regular arrangements up to completely ordered monolayers of molecules is denoted as molecular

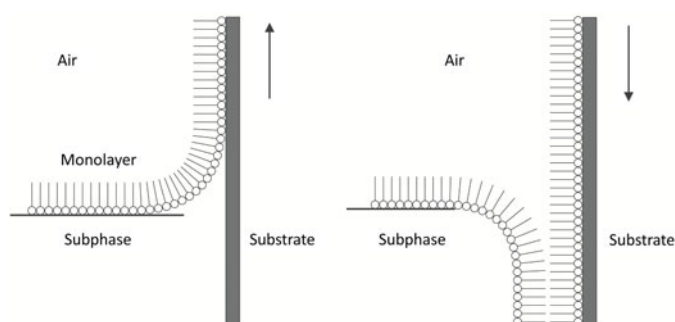


Fig. 4. Deposition of Langmuir-Blodgett film on substrate (left: monolayer, right: multilayer). Reprinted with permission from reference [16] (© IOP Publishing Ltd, 2001).

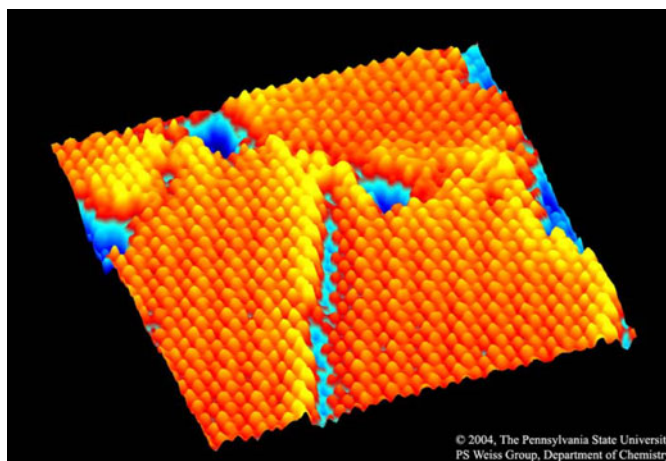


Fig. 5. Scanning tunneling microscopy image (15 nm × 15 nm) of Self-Assembled Monolayer of n-decanethiolate on Au {111}. Courtesy P S Weiss University of California, Los Angeles.

self-assembly [10]. Self-assembled monolayers (SAMs) (see Fig. 5), consisting of molecules containing a surface active binding group (headgroup) are widely investigated. The headgroup is accountable for chemisorption e.g. by covalent bonds on the substrate surface.

Typically, methylene groups form the spacer chain and the functional interface group determine the properties of the monolayer surface [25,26]. A schematic representation

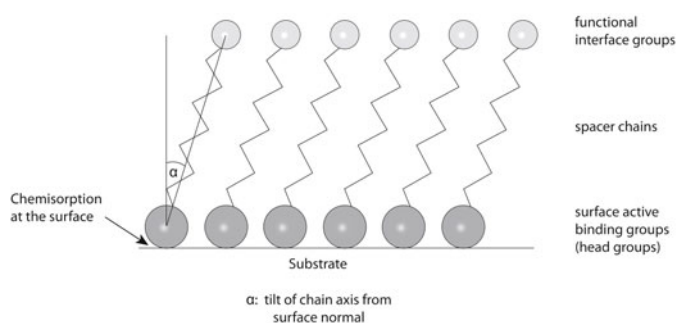


Fig. 6. Orientation of linear molecules on a metal surface, according to reference [27].

is shown in Figure 6. Moreover, spacer chains consisting of other organic groups, e.g., biphenyl, phenylene ethylene, anthracene are applied [27]. SAMs are formed by immersing a substrate into a uniform dilute solution of surface active material in an organic solvent (typically $1\ \mu\text{M}$ – $10\ \text{mM}$) [6,16,27]. Usually, ethanol serves as solvent, but also other solvents with sufficient solubility for the surface active material are common. The influence of the solvent type on the quality of the layer is small [14]. The surface active material adsorbs spontaneously and particularly on surfaces with low intrinsic roughness. Moreover, vapourized substances are deposited on the substrate out of the gas phase at low pressure [10,28]. The film formation process comprises the deposition followed by a rinsing or evacuation for removing excess material. Chemisorption leads to covalent or ionic bonding of the binding headgroup on a site of the substrate surface. Assuming some surface mobility by the chemisorption exothermicity the molecules are pushed close together on the surface [14]. The initially deposited monolayer becomes well-ordered as “crystalline” molecular assemblies after an assembly time of ~ 1 day [26]. Substrates of various shapes can be coated [29]. Generally, the orientation of the linearly elongated molecules deviates from the surface normal by a tilt angle that depends on surface material and molecule. N-alkanethiols on gold show tilt angles (see Fig. 6) near 30° , on silver near 10° [27]. Thioliates are approved for formation of SAMs on metals as Au, Pd, Ag, or Cu (see also Fig. 5). The sulphur surface active headgroup is attached to the metal surface. The structure of assembly of organic molecules on a surface is determined by the structure of the target surface which defines the distance between the individually deposited molecules. The interaction between the adsorbed molecules minimizes the free energy of the organic layer by van der Waals forces, hydrogen bonds and electrostatic interactions [10].

The formation of self-assembled monolayers on native silicon oxide and on bare Si surfaces for molecular electronics is reviewed by Aswal et al. [30]. A compilation of commonly deployed headgroups and substrates for the formation of SAMs on metals, oxides and semiconductors is given by Love et al. [27]; examples are presented in Table 1. The deposition of multilayered organic-inorganic hybrid films is feasible. Films containing

Table 1. Headgroups of molecules for SAM and the corresponding substrates. Reprinted with permission from reference [27] (© 2005, American Chemical Society).

Headgroup	Substrate	Reference
-OH	Si-H Si SiO _x	[31,32] [33] [30]
-COO-/-COOH	Ti/TiO ₂	[34]
-NH ₂	FeS ₂ Mica	[35] [36]
-C≡N	Ag, Au	[37]
-SH	Ag, Au, Cu Pt Zn	[38] [39] [40]
-CSSH	Au	[41]
-SeH	Ag Au	[42] [43]
≡P	FeS ₂	[35]
-N≡C	Pt	[44]
-SiX ₃ X = H, Cl, OCH ₂ CH ₃	HfO ₂	[45]

alternating silicon oxide and alkyl chains are formed based on 15-hexadecyltrichlorosilane (HTS) [46].

It is noteworthy that commonly self-assembled monolayers consist of molecules in upright positions. However, they can be assembled from molecules attached flat to the surface, too [47–49] (Fig. 7). Thus, also planar molecules with extended π -systems [10] physisorbed at surfaces can build two-dimensional supramolecular systems. Such molecular architectonics are systematically investigated both, on metal surfaces [50] and on thin insulating films [51]. Yet, the distribution of molecules on dielectric surfaces is much less investigated, although the functionalization of dielectric surfaces e.g. glass, polymers etc. holds many applications [47,49].

The variety of functional head groups opens up opportunities for a huge number of applications for SAMs. The list includes films that control the surface wettability, protective coatings (corrosion protection), tribological coatings, adhesion promotion, surface passivation, and interface engineering. SAMs serve as model systems for surface chemistry or as surfaces for biomedical purposes, e.g., to provide interaction with biological cells. Moreover, SAMs allow lateral structuring, e.g., to control the surface properties of electrodes for electrochemistry, cell interactions and molecular electronics [25–28,30,52]. Some examples shall be listed here: a gate dielectric of a 2.6 nm thick self-assembled monolayer of docosyltrichlorosilanes was used in polymer-thin-film transistors [53]. Organic SAMs are applied also for gate dielectrics on AlO_x and HfO₂ [54]. SAMs can serve as surfaces of biosensors [55]. For instance, ferrocenyl hexadecane thiol and aminoethanethiol SAMs are sensitive for the detection of glucose oxidase [56] and DNA [57].

SAMs can be modified by various methods: X-ray photons, UV-photons, ions, electrons, neutrals, and plasmas have been reported [58] and references therein or [59–61].

Table 2. SAM technique and Langmuir-Blodgett technique (see also [55]).

	SAM	LB
Surface bonding	Near equilibrium process, chemisorption	Nonequilibrium process, physisorption
Substrate	Only selected substrates chemical bond necessary	No requirements on substrate surface
Precursor	Specific headgroups, suitable for chemisorption required	Any long chain amphiphilic molecules
Solubility	SAM formation restricted to solubility of precursor molecules in the solvents	No solubility of precursor in the subphase
Stability	Densely packed and oriented films are thermodynamically stable and robust due to chemisorption	Transfer of the Langmuir film to the solid surface may change the structure of the monolayer due to weak physisorption
Interface for molecular alignment	Solid-liquid or solid-air interface	Liquid-air interface

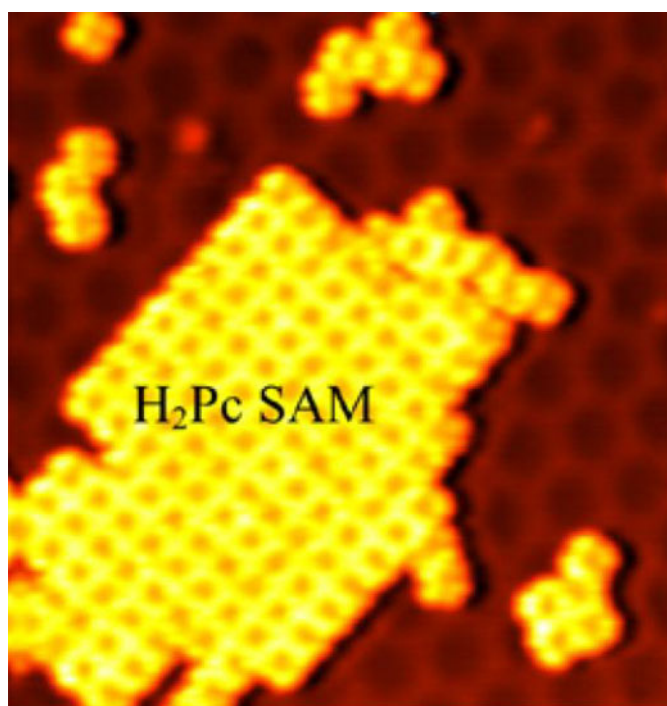


Fig. 7. Exemplary SAM film of H₂Pc molecules deposited flat on a Pb(111) surface (Scanning tunnel microscope image, shown dimension: 28 nm × 27 nm). From reference [48] (© IOP Publishing. Reproduced by permission of IOP Publishing. All rights reserved.)

The treatment of n-dodecanethiol films on Au substrate is investigated in a low density ($\sim 10^6$ electrons/cm³) downstream Ar or N₂ plasma ($p \approx 10^2$ Pa) containing a low O₂ concentration. The oxygen-derived radicals react faster with the S-Au interface than by oxidation of the alkyl chains [62]. Functionalization of highly ordered

monomolecular C₁₈ aliphatic layers occurs in O₂ low pressure (6 Pa) DC plasma pulses between 0.1 and 2 s [60].

Self-assembly of diblock copolymers on surfaces may lead to well-defined patterned structures [63–65]. For example, Mansky et al. [66] reported the formation of hexagonally packed arrays of hollow polybutadiene cylinders in a polystyrene matrix using polystyrene-butadiene diblock copolymer. An oxidative treatment by ozone creates a thin polystyrene film with a periodic array of cylindrical holes with size of 13 nm. Such polymer patterned surfaces can be used as nanolithography masks (diblock-copolymer nanolithography).

A comparison between self-assembly and Langmuir-Blodgett techniques for thin film deposition is given by Vijayamohan and Aslam [55] and summarized in Table 2.

3 Self-limiting deposition procedures

3.1 Atomic layer deposition (ALD)

A key method for the conformal deposition of defect free¹, ultra-thin films is atomic layer deposition (ALD), that has been derived from atomic layer epitaxy, (ALE) [67]. Extensive reviews on this topic are given by [68] and updated in [69], or [11,70]. ALD has been developed to create inorganic films with excellent step coverage and conformal coating of structured surfaces. The need for those thin, conformal films has been triggered largely by the semiconductor industry to fill trenches and other 3-D structures of high aspect ratios. The reactions between precursor and reactant are initiated by thermal energy (thermal ALD) as in conventional chemical vapour deposition. However,

¹ T. Bülow, H. Gargouri, R. Rudolph, S. Hamwi, W. Kowalsky, 7. ThGOT Thementage Grenz- und Oberflächentechnik, September 2011.

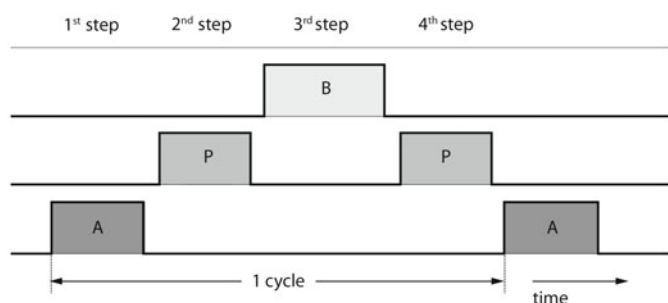


Fig. 8. Sequence of process steps as indicated by time dependent flows of purge gas P or evacuation and reactants A, B in a conventional ALD reactor. The position of the target is fixed in relation to the gas inlet. See also [71].

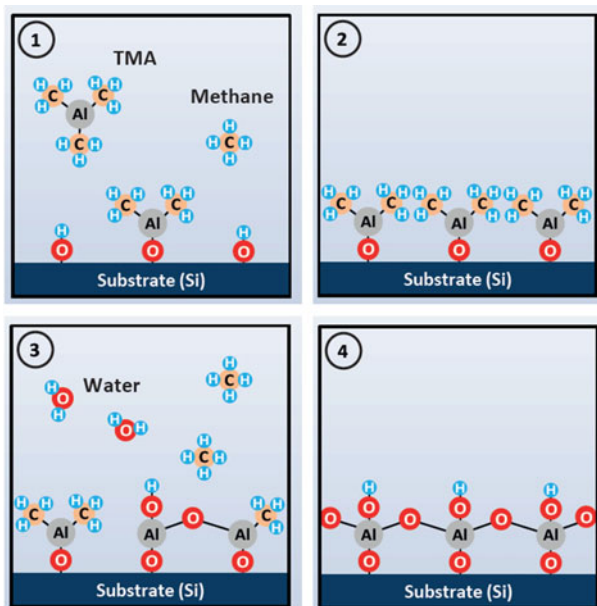


Fig. 9. ALD cycle using TMA and water vapour: 1 – TMA chemisorption, 2 – Purging step, 3 – Water chemisorption, 4 – Purging step.

different from CVD, the ALD technique uses sequential self-terminating surface reactions. Chemical volume reactions between the precursor molecules are excluded.

An accustomed process is the thermal deposition of Al_2O_3 layers described in detail by [68]. The four characteristic process steps of one reaction cycle to deposit Al_2O_3 using trimethyl-aluminium (TMA: $\text{Al}(\text{CH}_3)_3$) and water vapour (H_2O) as precursors are the following (Figs. 8 and 9):

1. In a *first step*, the gaseous precursor $\text{Al}(\text{CH}_3)_3$, the first reactant, is pulsed into the reactor chamber. The polar precursor molecules are chemisorbed on an OH-group terminated surface and cover the whole surface, also in trenches or other 3-D structures. The chemisorption terminates if all sites are occupied.
2. In a *second step*, all remaining, non-bonded precursor molecules and volatile reaction products are removed from the process by purging or evacuation.

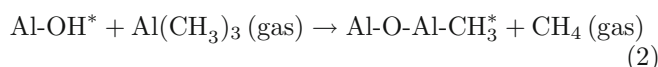
3. By a *third step*, the second reactant (H_2O vapour in this case) is pulsed into the reactor and similarly covers the substrate surface in a self-terminating way.
4. A *fourth step* again removes excess reactant along with volatile reaction byproducts by purging or evacuation, leaving an OH terminated surface ready for the next cycle.

Repeated reaction cycles lead (in an ideal case) to a film growth monolayer by monolayer.

The gross reaction for thermal ALD of Al_2O_3 is [68,70]



consisting of two self-limiting half reactions at the surface (* indicates surface sites)



Note that the above reactions (2) and (3) are written not balanced [72]. Figure 9 illustrates the surface processes for one cycle of Al_2O_3 -ALD.

Provided that the precursor dose (given by pulse duration and partial pressure) in each half reaction is above the saturation dose, the growth per cycle (GPC) is independent on the dose (Figs. 10 and 11, [73,74]), as well as on the corresponding purging times. In the example for TMA described there, a few ten milliseconds precursor pulse time provides sufficient molecules to saturate the substrate surface. The same is valid for the dependence on the vapour pressures of both reactants as shown for the deposition per cycle for the $\text{Al}(\text{CH}_3)_3/\text{H}_2\text{O}_2$ process in Figure 11. The self-terminating nature of the process effectuates that each reactant molecule occupies only one active surface site.

The self-terminating half reactions at the surface along with the absence of volume chemical reactions result in excellent uniformities over large areas and produce nearly one-to-one conformity of ALD films, even for aspect ratios (AR) of 1000 and beyond [11]. These problems are treated in detail by Elam [75]. Starting with a discussion of models considering the reaction time of surface processes and Knudsen diffusion inside the holes, Monte Carlo simulation examples are presented of ALD in structures with high aspect ratio: trenches, micromechanical systems (MEMS) (AR 10), membranes AR 100, silica gel $AR > 1000$.

The thickness uniformity (deviation from the mean value of the film thickness) of Al_2O_3 films, e.g., on 8'' silicon wafers is well below 1.5%. Figure 12 depicts the thickness distribution for such an Al_2O_3 layer as measured by spectroscopic ellipsometry².

Representative values of the GPC for Al_2O_3 are 0.8 Å/cycle with cycle times of only 2 s to attain uniform films (Fig. 10).

² H. Gargouri, F. Naumann, R. Rudolph, M. Arens, Atomic Layer Deposition (ALD) of ultra-thin and high conformal layers. 8. ThGOT Thementage Grenz- und Oberflächentechnik, September 2012.

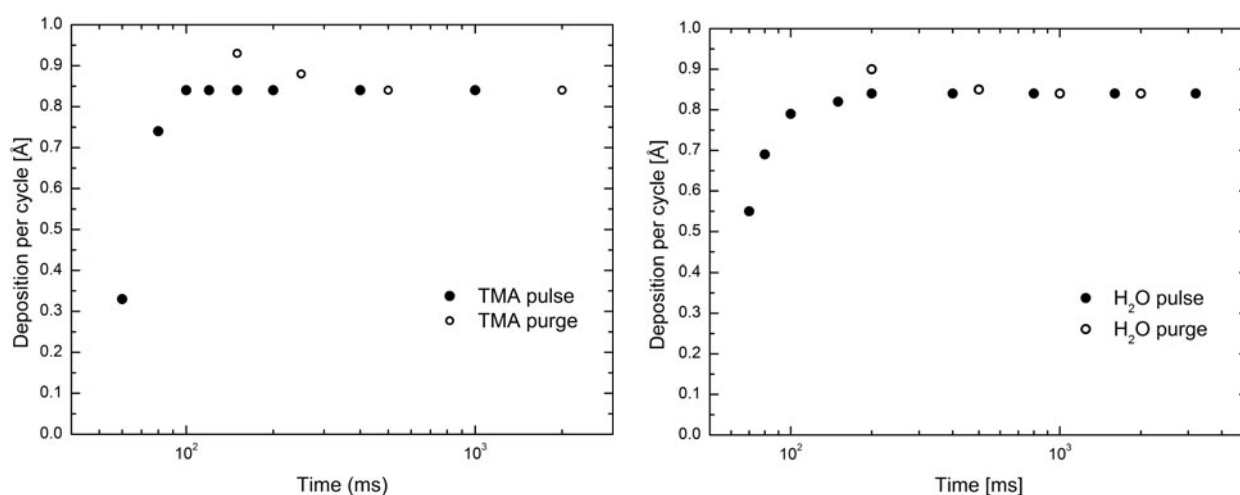


Fig. 10. Deposition per cycle of the $\text{Al}(\text{CH}_3)_3/\text{H}_2\text{O}$ process in dependence on the reactants (TMA and H_2O) and purge pulses. Reprinted from reference [73] (© 2002, with permission from Elsevier).

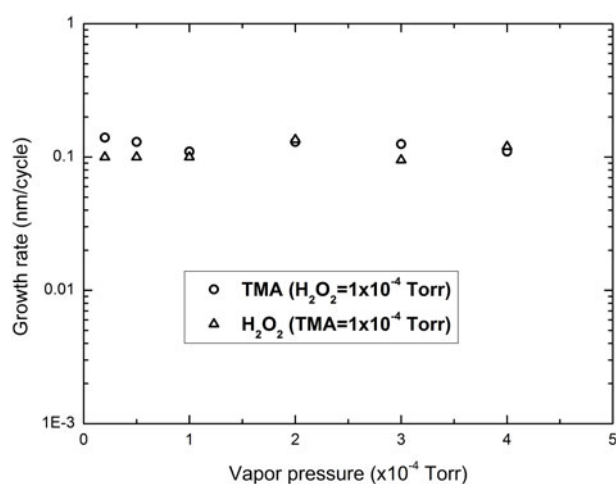


Fig. 11. Deposition per cycle of the $\text{Al}(\text{CH}_3)_3/\text{H}_2\text{O}_2$ process in dependence on vapour pressures of reactants. Reprinted from reference [74] (© 1994, The Japan Society of Applied Physics).

In reality, the assumption of an ideal monolayer growth can be violated. One main reason for that is the size of the precursor molecules. For instance, the number of TMA molecules necessary to cover a surface is smaller than the number of Al atoms to occupy all Al sites in a monolayer of Al_2O_3 .

Thus, after replacing the CH_3 groups by O the formation of a monolayer will remain incomplete [68]. Detailed investigations also show that the growth rate per cycle is not constant, especially for the first cycles. This growth inhibition depends on the reactants, the surface and the reaction temperature. Some observations were explained by island growth of the atomic layer [76,77].

A multitude of precursors have been developed to deposit ALD films from different materials. Requirements for precursor candidates are [78]:

1. Precursors must be volatile in the relevant temperature range.

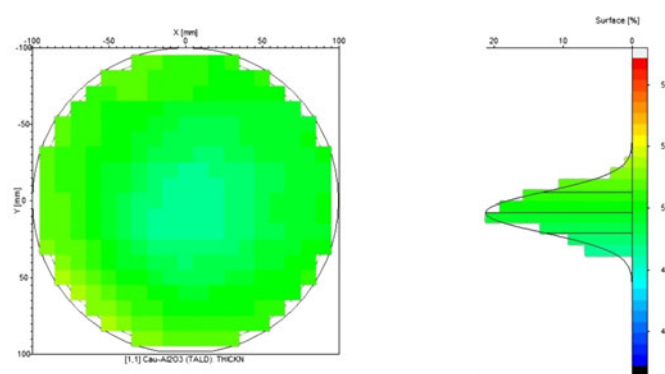


Fig. 12. Thickness uniformity of an ALD Al_2O_3 film on 8'' Si substrate (substrate temperature 200 °C, cycle time 4 s, GPC 0.8 Å/s, refractive index at 632.8 nm: 1.631).

2. They must be stable, must not decompose or undergo chemical reactions with other molecules of the same compound in the relevant temperature region.
3. The gas-solid reactions have to be self-terminating,
4. Good adsorption or reactivity with surface sites is a prerequisite.
5. The reactivity against the counterpart precursor must be sufficient.
6. The substrate must not be etched by the precursor.

The precursor is introduced into the reactor as vapour or as liquid injection of the precursor in an appropriate solvent (Liquid injection atomic layer deposition, LIALD) [79,80]. Typical applied precursors are summarized in Table 3 [68]. A compilation of ALD processes is listed in Table 4.

ALD is applied in microelectronics, for coating of nanoparticles, soft materials such as polymers, and biomaterials and for the generation of biocompatible surfaces [11]. The usage of Al_2O_3 as passivation layer is reported in [99] where the film prevents oxidation and aging of slanted columnar thin Co films. The deposition of high- k dielectrics as HfO_2 [100], $\text{Al}_2\text{O}_3\text{-Ta}_2\text{O}_5$ [101],

Table 3. Typical ligands L of reactants ML_n used in ALD. M indicates the central atom, usually metal. Organometallic compounds are distinguished by direct metal-carbon bonds. Reprinted with permission from reference [68] (© 2005, AIP Publishing LLC).

Inorganic						
M	$M-F$	$M-Cl$	$M-Br$	$M-I$	$M-H$	$M=O$
(no ligand)	Fluoride	Chloride	Bromide	Iodide	Hydride	Oxo
Organic						
<i>Organometallic</i>						
Methyl (Me)	Ethyl (Et)	Isopropyl (Pr)	Allyl (Ay)	n-Butyl (ⁿ Bu)		
Isobutyl (ⁱ Bu)	Tert-butyl (^t Bu)	Neopentyl (Np)	Cyclopentadienyl (Cp)	Methylcyclopentadienyl (CpMe)		
Pentamethylcyclopentadienyl (CpMe ₅)	Ethylcyclopentadienyl (CpEt)	Tri-isopropylcyclopentadienyl (Cp <i>i</i> Pr ₃)	Trimethylsilylcyclopentadienyl [Cp(SiMe ₃)]			
<i>Complex-organic compounds</i>						
Methoxy (OMe)	Ethoxy (OEt)	Isopropoxy (O ⁱ Pr)	Isobutoxy (O ⁱ Bu)	Tert-butoxy (O ^t Bu)		
1-Methoxy-2-methyl-2-propoxy (mmp)	Dimethylaminoethoxy (dmae)	Acetylacetonato (acac)	2,2,6,6-Tetramethyl-3,5-heptanedionato (thd)			

Table 3. Continued.

Organic					
Complex-organic compounds					
1,1,1,5,5,5-Hexafluoroacetylacetonato (hfac)	Octan-2,4-dionato (od)	1-(2-Methoxyethoxy)-2,2,6,6-tetramethyl-3,5-heptanedionato (methd)	2-Amino-pent-2-en-4-onato (apo)		
Acetoxy (OAc)	Dimethyl-amido (NMe ₂)	Ethylmethyl-amido (NEtMe)	Diethyl-amido (NEt ₂)	Bis(trimethylsilyl)amido [N(SiMe ₃) ₂]	Tert-butylimido (N ^t Bu)
N,N'-diisopropylacetamidinato (iPrAMD)	N,N'-ditertbutylacetamidinato (tBuAMD)	1,10-phenanthroline (phen)	Dimethylglyoximato (dmg)	Diethyldithiocarbamato (dedtc)	

ZrO₂-Gd₂O₃ [102] allows the formation of capacitors with high capacitance and low leak currents.

Moreover, ALD receives growing attention in applications such as for the deposition of passivation layers on solar cells, for diffusion barriers for OLEDs and thin film photovoltaics. These applications require high-throughput and low-cost techniques which are preferably suitable for in-line processes [71]. One instructive technical development towards the requirements above represents the so-called spatial ALD. Opposed to conventional ALD, where the substrate remains at a fixed position and the flow of reactants is time dependent, spatial ALD exposes the substrate subsequently to the appropriate reactant or purge flow by controlled back and forth movement of the substrate. The flows are each constant over time as demonstrated in Figure 13. Several constructive solutions are reviewed by Poodt et al. [71]. A technical approach to

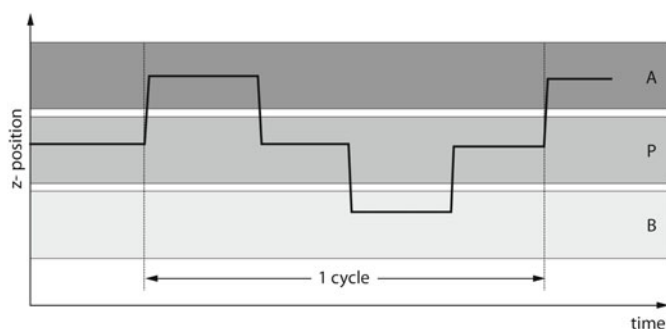
an atomic layer deposition system for the production of ZnO thin film transistors is shown in Figure 14 [103]. In particular, this system operates under normal pressure conditions.

For spatial ALD, the process is based on relative movement of the gas supply device against the target. By repetitive movement each target region is alternatively exposed to reactant A, followed by the purge gas flow P and subsequently with reactant B. Without lateral motion no chemical reaction can proceed and hence no film develops.

The main advantage of spatial ALD is the reduction of the purge time because the idle volume is considerably smaller than in conventional ALD. The tight construction dispenses with otherwise larger reactor wall areas. Hence, the target itself represents the major part of the surface and the reactor wall area which is ineffective for

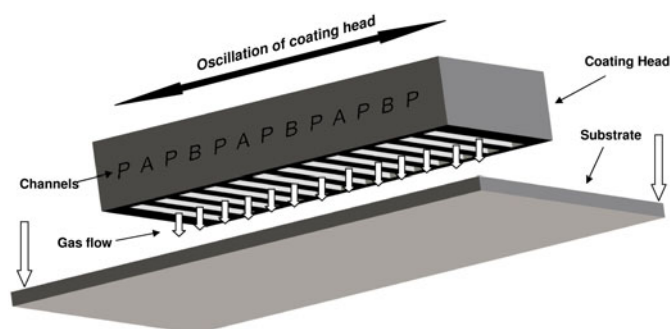
Table 4. Examples of ALD processes, see also [68,69].

	Compound	Reactant A	Reactant B	Reference
Mg	MgO	MgCp ₂	H ₂ O	[81]
Al	Al ₂ O ₃	Al(CH ₃) ₃	H ₂ O	[82]
Ir	Ir	Ir(acac) ₃	O ₂	[83]
	IrO ₂	Ir(acac) ₃	O ₃	
Mo	Mo	MoF ₆	Si ₂ H ₆	[84]
Co	Co ₃ O ₄	CoI ₂	O ₂	[85]
	TiO ₂	TiCl ₄	H ₂ O	
Ti	TiN	TiCl ₄	NH ₃	[87]
	TiN	Ti(NC ₂ H ₆) ₄	NH ₃	[88]
Cu	Cu	Cu(OCHMeCH ₂ NMe ₂) ₂	Et ₂ Zn	[89]
Ru	RuO	Ru(CpEt) C ₄ H ₄ N (pyrrolyl)	O ₂	[90]
	RuO ₂	Ru(CpEt) ₂	O ₂	[91]
	Ta ₂ O ₅	Ta (OEt) ₅	H ₂ O	[92]
Ta	TaN	Ta (dmae) ₅	NH ₃	[93]
	Ta ₃ N ₅		CH ₃ (NH)NH ₂	
	NbTaO _x	TaF ₅ and NbF ₅	H ₂ O or H ₂ O/O ₃	[94]
Pt	Pt	Pt(CpMe)(Me) ₃	Air	[95]
W	WS ₂	WF ₆	H ₂ S	[96]
	W	WF ₆	Si ₂ H ₆	[97]
Zr	ZrO ₂	Zr[N(CH ₃)C ₂ H ₅] ₄	O ₃	[98]

**Fig. 13.** Spatial ALD. Z: position of a target area in relation to the corresponding gas inflow channel in dependence on time. A: flow of reactant A, B: flow of reactant B, P: flow of purge gas (after [71]).

the process is minimized. This leads also to a significantly reduced consumption of often expensive reactants.

Along with the unrivalled advantages of ALD mentioned already at the beginning of this section, like low defect density, excellent conformity and thickness control that allow the deposition of uniform films over large and 3D substrates, there are some drawbacks. The chemistry of the selected precursor and reactants limits the process to a small parameter window. In particular, the processes often require temperatures above 200 °C or even above 300 °C, thus hampering the usage of most polymeric substrates. Moreover, the growth rates are comparably small and the process requires two process steps. The required precursor vapor pressure restricts the reac-

**Fig. 14.** Coating scheme of spatial ALD at atmospheric pressure (after [103]). During operation, the substrate is moved directly below the coating head. In this sketch, for better visibility of the gas channels, the substrate is drawn in a lowered position.

tants and the usage of metal organic precursors may result in carbon impurities.

A notable combination of ALD and self-assembling thin film deposition is the technique for nano-patterning by area-selective atomic layer deposition [104–106]. Combination of SAMs and ALD can generate organic-inorganic composite films. The tail group of the SAM governs the chemistry of the surface. Hence, a hydrophilic substrate surface can be changed into a hydrophobic surface by, e.g., the CH₃ tail groups of the SAM molecules or vice versa. ALD precursors with different reactivity to various tail groups can be utilized for surface patterning. SAMs can enhance the growth of inorganic films

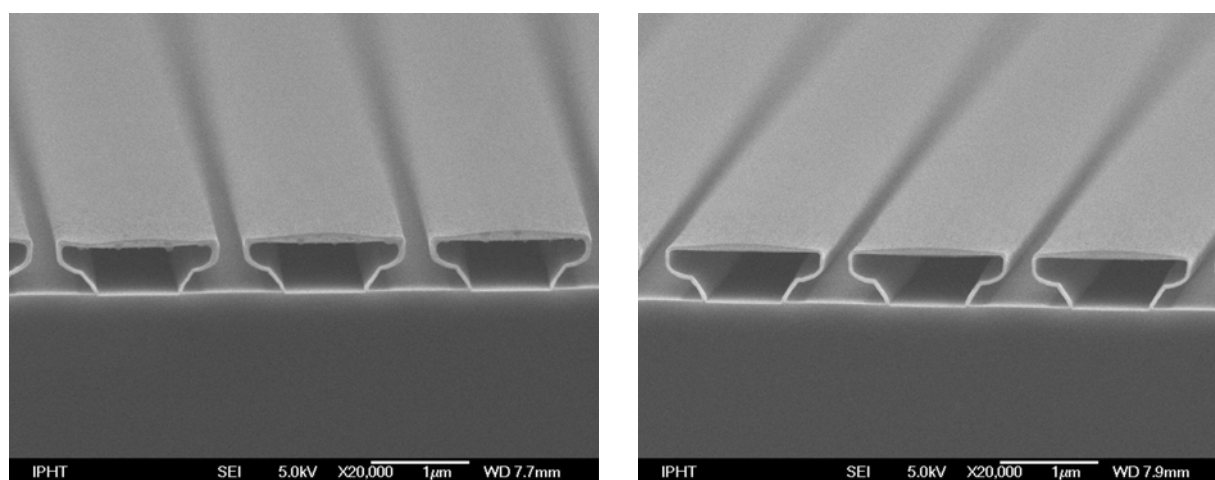


Fig. 15. Conformal deposition of Al_2O_3 on photoresist. Left: thermal ALD, right: PA-ALD. To obtain a clear contrast the resist was removed thus creating hollow Al_2O_3 structures. The seemingly higher thickness on top of all structures originates from subsequent Pt sputter deposition (with courtesy of IPHT Jena, Germany).

or can block the growth of such films, i.e. they act as mask. For instance, trimethylaluminum used as precursor for Al_2O_3 ALD exhibits a higher chemical reactivity on a hydrophilic surface than on a hydrophobic [107]. Therefore, a structured SAM surface can generate and control patterned ALD. SAMs are patterned using various methods, e.g. applying microcontact printing (μCP), photolithography, electron beam, ion bombardment, scanning probe microscopy [108,109].

3.2 Plasma enhanced atomic layer deposition (PE-ALD)

As in conventional chemical vapour deposition, the input of thermal energy is necessary to induce the chemical reactions required for thin film growth in conventional, thermal ALD. In contrast, during plasma assisted or enhanced plasma ALD (PE-ALD) this energy input is delivered by electrical discharges and the thermal processes are replaced by plasma activation. In the electrical discharges of relevance here, the primary energy transfer necessary to activate the gaseous species is provided by inelastic collisions with electrons. In these typically non-thermal plasmas the collision rate remains too low to attain thermal equilibrium and the gas possesses much less mean energy (10^{-2} – 10^{-1} eV range) as the electrons (with mean energies typically between 1 and 3 eV). The gas and substrate therefore remain at comparably low temperatures. Non-equilibrium processes are predominant, the collisions produce electronically excited atoms and molecules or unsaturated radicals by dissociation and ions by ionization [110,111]. Whereas ions play only a secondary role for the volume chemistry due to normally prevailing small ionization degrees of typically 10^{-3} or less, even a small number of energetic ions can influence the surface processes significantly. Detailed reviews of PE-ALD are provided by references [112,113].

The plasma activation of the reactants allows the replacement of chemically active reactants by non-reactive

gases or vapours which are activated by formation of radicals, e.g., O atoms in O_2 plasmas. PE-ALD allows the decrease of process temperature, opens the process window and extends the choice of precursors. Moreover, decreased impurities and enhanced deposition quality is reported [114]. Another advantage is the deposition of materials in elementary form, which is difficult by thermal ALD [69,70]. The most notable disadvantage may be a reduced conformity for high aspect ratios, because radicals of the reactant gas generated by plasma may suffer loss processes during their transport towards the surface, which can lead to inhomogeneous deposition particularly in deeper trenches. However, for intermediate aspect ratios no significant difference is observed comparing the conformity of a thermal ALD Al_2O_3 film with a PE-ALD film on similar geometry as shown in Figures 15 and 16. The PE-ALD of Al_2O_3 in a macropore structure by 700 ALD cycles is presented in Figure 16 [115]. The pores have a diameter of 2–2.5 μm and a depth of 19 μm , and an aspect ratio of ~ 8 . The film thickness on the top surface was 83 nm, and on the sidewall and the bottom of the pores 80 ± 3 nm. This picture demonstrates the conformity of PE-ALD.

Another critical issue is related to a possible plasma induced damage of the deposited film [116]. Such damage is circumvented by usage of plasma sources which deliver a flux of neutral radicals and diminish detrimental exposure to ions or UV radiation (remote or true remote plasmas).

PE-ALD usually operates under vacuum conditions. Apart from the items common for plasma vacuum devices like appropriate plasma source, vacuum chamber, pumping unit valves, and pressure control, the reactor systems (see Fig. 17) for PE-ALD are equipped with a heated substrate holder and gas management systems for (1) precursor and (2) reactant and/or purge gas that allow specifically for a fast and controlled, pulsed gas inlet and exhaust. Additional facilities for control of thin film growth, gas phase composition, and temperature control ensure reproducible operation conditions.

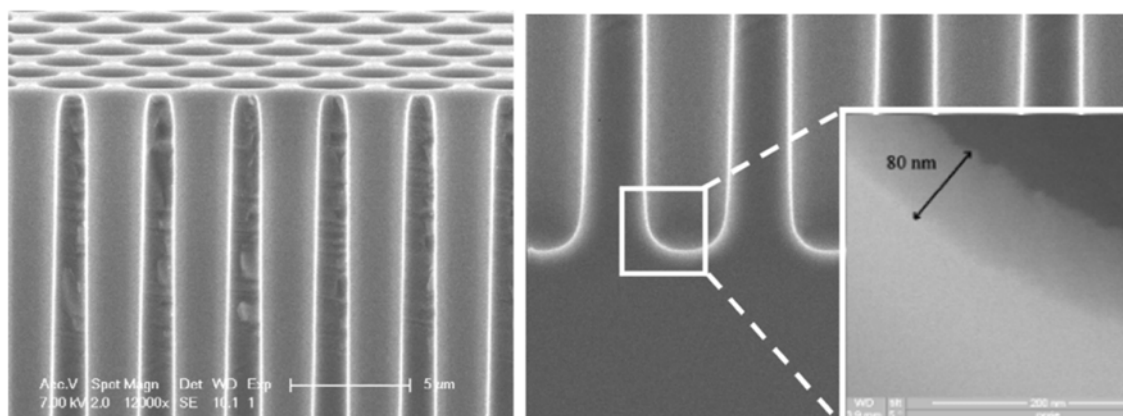


Fig. 16. SEM images of macropores coated with Al_2O_3 by 700 plasma assisted ALD cycles. Aspect of ratio the pores ~ 8 , diameter 2–2.5 μm , depth 19 μm . Reprinted from reference [115] (reproduced by permission of The Electrochemical Society).

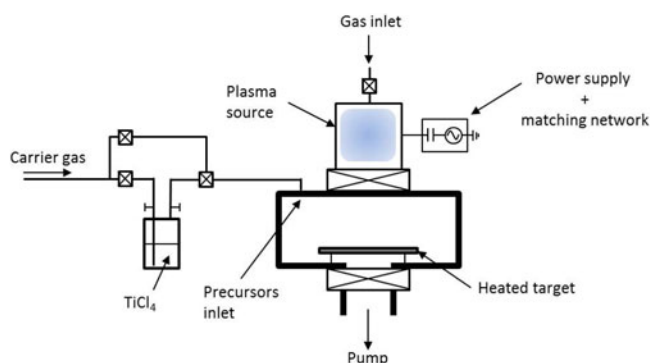


Fig. 17. PA-ALD reactor for deposition of TiN with remote plasma source.

Schemes of reactor types are shown in Figure 18. The discharge can be operated as dc, ac, rf or MW plasma and generated either directly in contact with the substrate (Fig. 18a) or remotely (Figs. 18b and 18c), with the plasma source placed upstream in some distance from the substrate. Moreover, an interaction of the precursor with the discharge directly in the volume can be suppressed by the time regime of the process. In both cases (Figs. 18b and 18c), the influence of energetic ions is suppressed and the species that react with the surface are predominantly free radicals and excited neutral atoms or molecules. If the plasma region is in direct line of sight to the target, than also the influence of photons should be considered (Fig. 18b).

The type illustrated in Figures 18c and 19 is referred to as true remote plasma source. It could be shown for such a plasma source (Fig. 18b) that for typical flow conditions and metal organic PE-ALD, apparent transport of precursor into the excitation region is blocked by reducing the diameter of the gas inlet to 5 mm,³ thus leading to a metal

PE-ALD process with enhanced purity of the coating. A specific version of the plasma source shown in Figure 18b is equipped with an additional screen between the plasma and the substrate to protect the substrate against UV and ions, transforming this source into a true remote plasma (Fig. 19).

The PA-ALD process is conducted in coordinated steps:

1. Precursor is introduced temporally controlled into the reactor and is absorbed at the substrate.
2. Precursor flow is stopped; non-absorbed, excess precursor is removed from vessel by purging with purge gas/carrier gas.
3. After introducing reactant gas (e.g. O_2), gaseous reactants are generated by the discharge. These react with adsorbed precursor.
4. Plasma is turned-off.
5. Volatile reaction products are removed by purging.

Each cycle leads to the deposition of one monolayer.

Such cycles are demonstrated in Figure 20 for PE-ALD of TiN formation [118].

The plasma enhanced TiN deposition using TiCl_4 as precursor and a N_2/H_2 plasma for generating the reactants represents a prime example for a process that is not feasible by conventional thermal ALD. H and N radicals are considered the key reactive species generated by the discharge. The chlorine is removed from the adsorbed TiCl_4 molecules by H atoms by formation of HCl. The N radicals react with the Ti surface forming TiN. According to the sequence above, the substrate is initially exposed to the precursor TiCl_4 with the reaction chamber being separated by closed valves from plasma source and pump. Ar flow dilutes the TiCl_4 vapour to avoid corrosion of reactor and lines. Furthermore, Ar purges the non-adsorbed part of TiCl_4 from the chamber after the exhaust valve is opened. In the next step, the valve that connects the N_2/H_2 plasma source with the chamber is opened and allows the plasma to interact with the target. After a short period, the plasma is switched off and the reaction gas acts as purge gas finishing one cycle.

³ H. Gargouri, K. Wandel, F. Naumann, H.E. Porteanu, R. Gesche, R. Rudolph, M. Arens, Microwave Microplasma Source For Plasma Enhanced Atomic Layer Deposition, Pt-16. 16. Fachtagung Für Plasmatechnologie Greifswald, February 2013.

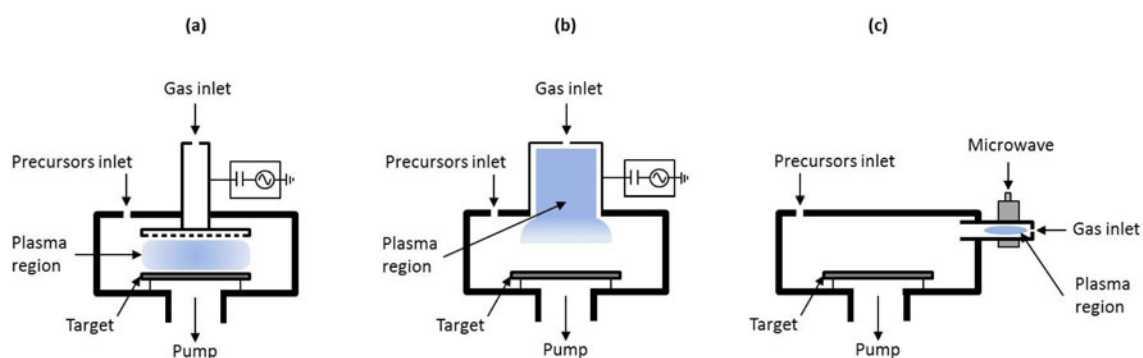


Fig. 18. PE-ALD reactors with different positions of plasma and target. Plasma in contact with target (a), remote plasma in contact with target (b), target in contact only with plasma generated radicals (c) (according to [117]).

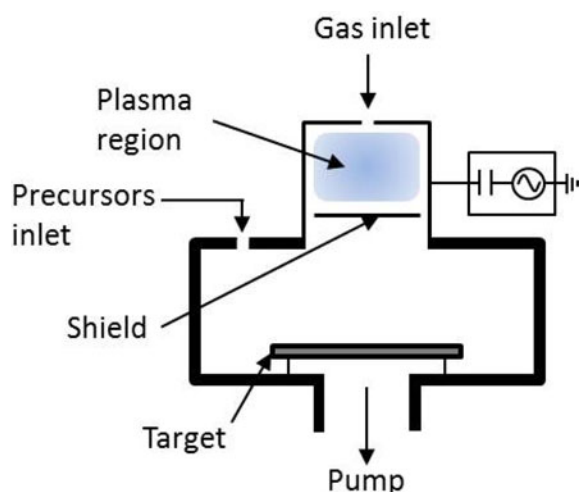


Fig. 19. PE-ALD reactor with a true remote plasma source equipped with additional screen.

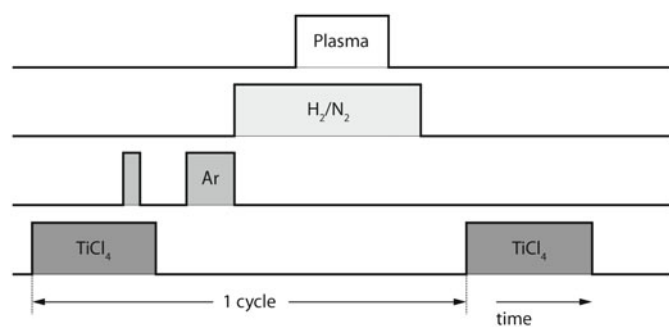
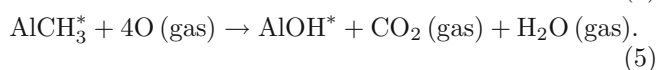
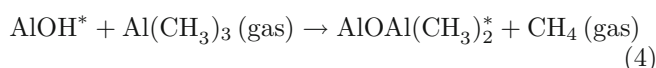


Fig. 20. PE-ALD cycle for TiN-deposition from TiCl_4 as precursor. Ar: precursor carrier and purge gas. Reprinted from reference [118] (reproduced by permission of The Electrochemical Society).

Another exemplary PE-ALD process is the formation of Al_2O_3 using a plasma process with $\text{Al}(\text{CH}_3)_3$ and O_2 . The surface chemistry of this process is described by [119]



It is noteworthy that PE-ALD of Al_2O_3 films has been achieved already with plasma generated O atoms at temperatures as low as 25°C [120]. Figure 21 shows some properties of PE-ALD Al_2O_3 films at reduced substrate temperatures and typical plasma pulses of 5 s. The decreasing refractive index when lowering the temperature is interpreted as lower film density. Moreover, an increased carbon content could be observed using energy dispersive X-ray measurements (EDX).

The requirements of the precursors for PE-ALD are practically the same as for ALD. They must be volatile at an experimentally easy to handle temperature. Thermal stability in the processing temperature range is necessary. Polar molecules are required, which in addition should possess a sufficient reactivity with the surface. Another mandatory prerequisite of the molecules is their property of self-termination [68].

Metal halogenes and metal organic compounds serve as precursors for the deposition of metals, metal oxides and inorganic metal compounds. The deposited materials and the applied precursors are compiled in Table 5 along with the reactant gases and the field of application.

Two types for transport of precursors into the reactor are discussed [70], direct transport by throttled pumping [121–123] or transport by a carrier gas [124–126]. Depending on the vapour pressure of the precursor a heating of the source may be required.

As listed in Table 5, applications of PE-ALD films can be found in micro- and nano-electronics. Pure metal films with low resistivity, acting as diffusion barriers and also as contact films for adhesion of other materials are reported. Metal oxide films forming high- k dielectric films are essential in micro-electronic devices as they allow dielectric films in capacitors with lower leak currents. Concerning the combination of ALD and SAM, as mentioned above, the application of PE-ALD has to take into account the modification of the SAM by the plasma [59,60,106].

3.3 Molecular layer deposition (MLD)

Whereas ALD techniques are restricted to the deposition of inorganic compounds or metals, in contrast, MLD allows also the deposition of organic, metal-organic, and

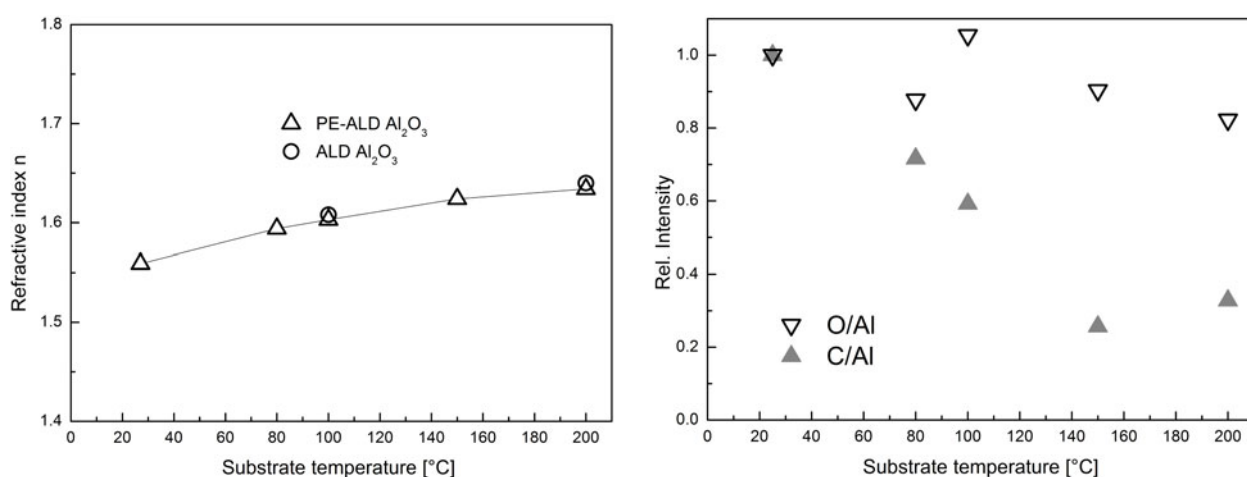
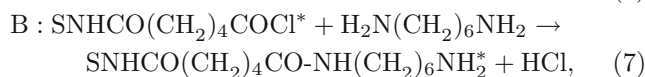


Fig. 21. Influence of the substrate temperature on the film properties of PE-ALD Al_2O_3 : left – refractive index at 632.8 nm; right – normalized EDX intensity ratios.

hybrid organic-inorganic polymer materials. A representative list is given in Table 6 [171–173]. Like thermal ALD, thermal MLD is based on sequential, self-limiting thermally initiated surface reactions. For instance, the deposition of a polyamide as nylon 66 is described by a repetitive sequence of the surface condensation reactions A and B [171,174].



where S denotes the substrate and * denotes surface species.

Furthermore, polymers like polyimide, polyimide-polyamide, polyurea and polyurethane are deposited by MLD procedures [171]. The use of three different precursors in a three step reaction opens up new possibilities of polymer deposition with new functionalities [171].

Examples of hybrid organic-inorganic film coating are “alucone” [175] and “zincone” [12] resulting from the reaction of diols as ethylene glycol with metal alkyls as trimethyl-aluminium and diethylzinc, respectively.

The MLD process is carried out by separately introducing the flow of carrier gas e.g. N_2 (pressure $\sim 10^2$ Pa) and of the reactants (~ 10 Pa) into the reactor. A longer purge time after each exposure cleans the volume from the non-absorbed reactants and purges volatile reaction products. One MLD cycle is given by the exposure time of each reactant and the purge process. Common deposition temperatures are in the region ~ 100 °C up to 200 °C. Observed growth rates per cycle are in the range of some 0.1 nm [171].

3.4 Plasma enhanced molecular layer deposition

Surface coating by repeated plasma-enhanced grafting and cross linking of molecular precursors [2] can be under-

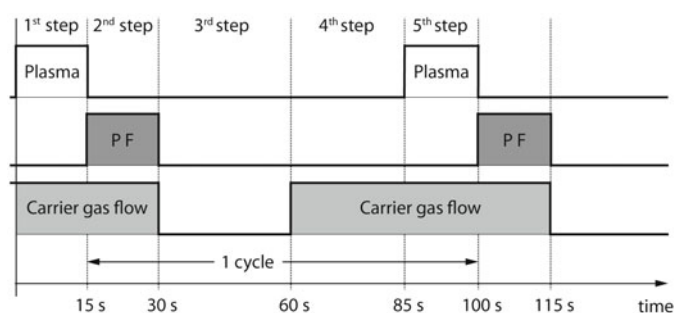


Fig. 22. Timing scheme of PE-RDG procedure of processing control parameters plasma power, precursor flow (PF), and carrier gas flow (according to [2]).

stood as a technique of plasma assisted molecular layer deposition.

The process of plasma enhanced repeated grafting deposition (PE-RGD) is characterized by chronologically controlled precursor flow and surface activation by plasma. The sequence starts by exposing the substrate surface by a plasma for cleaning and to initiate a surface activation. No thin film producing agents are transported to the surface during this phase, the plasma is just ignited in the carrier gas. The activation of the substrate surface generates metastable surface radicals or active sites which provide reaction partners for subsequent surface grafting reactions with monomer molecules.

The usual timing scheme of control parameters during PE-RGD is given in Figure 22. One cycle is described by five steps:

1. The first step comprises the plasma activation.
2. In the second step, after having switched off the discharge, the thin film producing agent (precursor) is mixed to the carrier gas flow.
3. At the beginning of the third step, the exhaust valve is closed, and the gas flow is stopped, thus allowing surface grafting reactions to proceed.

Table 5. PE-ALD of metals and metal compounds: Deposited materials, precursors, plasma process gases, and applications.

Material	Precursor	Gas	Application	Reference	
Ag	(2,2-dimethylpropionato)silver(I)triethylphosphine	H ₂	Low resistivity film	[127]	
Co	cyclopentadienyl isopropyl acetamidinato-cobalt	NH ₃	Low resistivity films,	[128]	
	(bis(N,N'-diisopropylacetamidinato)cobalt(II)			[129]	
	CoCp ₂			[130]	
	CoCp(CO) ₂			[131]	
Cu	copper(II)acetylacetonate	H ₂	Low resistivity film,	[61]	
	Cu-II(tetramethyl-3,5-heptanedionate) ₂			[132]	
				[133]	
Ir	Ir(EtCp)(COD)	NH ₃	Film with excellent thermal and morphological stability at 850 °C	[134]	
Ni	bis(dimethylamino-2-methyl-2-butoxo)nickel	NH ₃ or H ₂	Low resistivity film	[135]	
Pd	palladium(II)hexafluoroacetylacetonate [Pd-II(hfac) ₂]	H ₂ /N ₂	Film on polymer substrate 80 °C	[136]	
			Contact film for Cu deposition on TaN	[137]	
Ru	Ru[EtCp] ₂	N ₂ /H ₂	Cu diffusion barrier	[138]	
	CpRu(CO) ₂ Et			[139]	
	(eta 6-1-Isopropyl-4-MethylBenzene)			O ₂	[140]
	(eta4-CycloHexa1,3-diene)Ruthenium (0)			NH ₃	
Ta	TaCl ₅	H ₂	Cu diffusion barrier	[141]	
				[142]	
				[143]	
Ti	TiCl ₄	H ₂	Cu diffusion barrier	[144]	
				[143]	
Al ₂ O ₃	Al(CH ₃) ₃	O ₂	Corrosion protection,	[145]	
			passivation layer,	[124]	
			diffusion barrier,	[145,146]	
			gate dielectric	[147]	
Ga ₂ O ₃ Ga ₂ O ₃ -TiO ₂	[(CH ₃) ₂ GaNH ₂] ₃	O ₂	Gate dielectrics	[148]	
				[149]	
HfO ₂	HfCl ₄ tetrakis(dimethylamino)hafnium Tetraethylmethyl amino hafnium Hf(OH) ₃ NH ₂ Tetraethylmethyl amino hafnium	O ₂ /N ₂	High- <i>k</i> dielectric film	[150]	
		H ₂		[151]	
		Ar/O ₂ or		[117]	
		H ₂ O O ₂		[122,152]	
		O ₂		[126,153]	
La ₂ O ₃	tris(isopropyl-cyclopentadienyl)lanthanum La(EtCp) ₃	O ₂	Gate oxide	[154]	
		O ₃		[154,155]	
SiO ₂	bis-diethylamino-silane	O ₂	Dielectrics	[156] [157]	
SnO ₂	Dibutyltindiacetate	O ₂	Gas sensor	[158]	
TaN _x	Ta[N(CH ₃) ₂] ₅	H ₂ , H ₂ -N ₂ , NH ₃		[125]	
Ta ₂ O ₅	Pentakis(dimethylamino)tantalum	O ₂	Dielectrics	[120]	
				[159]	
TiO ₂	TiCl ₄ Tetrakis(dimethylamino)titanium Ti((OPr)-Pr-i) ₄ , Ti(Cp-Me)((OPr)-Pr-i) ₃ , TiCp*(OMe) ₃ Ti{OCH(CH ₃) ₂ } ₄	O ₂	Photocatalytic, superhydrophilic	[160]	
		O ₂		[161]	
		O ₂		[120]	
		O ₂		[162]	
		O ₂		[163]	
TiN	TiCl ₄	H ₂ /N ₂		[118,152]	
Va ₂ O ₅	Vanadyl-tri-isopropoxide	O ₂		[164]	
ZnO	(CH ₃) ₂ Zn	H ₂ O	TFT on flexible plastic substrate	[165]	
				[166]	
ZrO ₂	ZrCp ₂ (NMe ₂) ₂ ;	H ₂	Gate dielectrics TFT	[167]	
	ZrCp ₂ (η ² -MeNCH ₂ CH ₂ NMe)			[168]	
	Zirconium tertiary butoxide			O ₂	[169]
	Tetrakis(ethylmethylamino)zirconium			[170]	

Table 6. Examples of thermal MLD processes for formation of metal-organic, organic-inorganic hybrid and polymer films.

Product	Precursor 1	Precursor 2	Method	Application	Reference
Alucone AlOCH ₂ CH ₂ OAl	Al(CH ₃) ₃ , H ₂ O	Ethylene glycol OH-(CH ₂) ₂ -OH	N ₂ carrier and purge gas		[175]
Alucone alloys	Al(CH ₃) ₃ plus Ethylene glycol MLD step	Al(CH ₃) ₃ plus H ₂ O ALD step	(ALD:MLD) = 1:3 up to 6:1		[106]
Zincoxes (-ZnORO-) _n	Zn(CH ₂ CH ₃) ₂	Ethylene glycol OH-(CH ₂) ₂ -OH	N ₂ carrier and purge gas 90–170 °C		[12]
Vanadium[tetracyano ethylene] _x V[TCNE] _x	V(CO) ₆	TCNE	Evacuation between precursor exposure	Magnetic semi-conducting laminate	[176]
Organic-inorganic hybrid film, TiOPDA-TiO ₂	TiCl ₄ , H ₂ O	TiCl ₄ , 2,4- hexadiyne-1,6-diol, uv polymerization			[177]
Conformal organic-inorganic hybrid network polymer thin films (-AlO(C ₄ H ₈)O-) _n	Al(CH ₃) ₃ , H ₂ O	Hetrobifunctional glycidol		Gas separation, diffusion barriers	[178]
Polymer film formation	Pyromellitic dianhydride	2,4-diaminonitrobenzene or diaminodiphenyl ether	15 steps formed 10 nm film		[179]
Quantum wire and dot formation	Terephthalaldehyde	p-phenylenediamine			[180]
Poly(p-phenylene terephthalamide) thin film	Terephthaloyl chlorid	p-phenylenediamine			[181]
Nylon 66	Adipoyl chloride	1,6-hexanediamine			[174]

Table 7. Deposition conditions for various precursors and substrate materials (allyltrimethylsilane ATMS, hexamethyldisilazane HMDSN, dimethylaminotrimethylsilane, DMADMS, bis(dimethylamino)dimethylsilane BDMADMS); PEEK Polyetheretherketone, PS polystyrol [2].

Precursor	Precursor gas flow	Substrate	Carrier gas	Carrier gas pressure/gas flow	Plasma	Growth rate nm/cycle
ATMS	0.3 sccm	Silicone	Ar	5 Pa, 100 sccm	13.56 MHz	0.59
HMDSN		Glass			inductive	0.35
DMATMS		PEEK			coupling	0.62
BDMADMS		PS			50 Watt	0.45

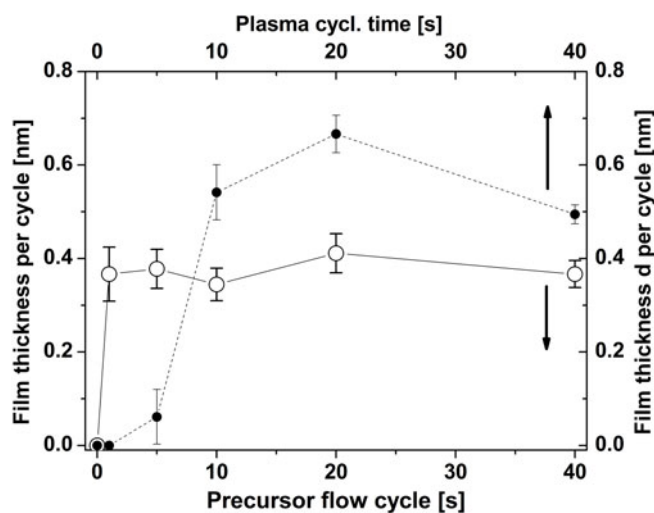


Fig. 23. Growth rate per cycle in as function of the precursor dosing time (open symbols, lower x -axis) and as function of plasma pulse length (solid symbols, upper x -axis), according to reference [2].

- In the fourth step, after grafting has ceased, the excess molecules, which haven't been grafted, are flushed away by opening the exhaust valve and engaging the carrier gas flow.
- During the fifth step the discharge is switched on again, to initiate a cross-linking of the attached molecules and form active surface sites anew, thus preparing the surface for another sequence.

This process sequence ensures that the precursor molecules are not exposed to the plasma during their transit between inlet and target. Hence, critical volume reactions cannot occur and only surface processes develop. The characteristic self-limiting nature is demonstrated by the self-termination of the precursor absorption on the surface as shown in Figure 23 by the constant growth rate per cycle as a function of precursor dosing time. Also, the dependence on the pulse duration of the applied power can be explained by the self-limiting property of the process. After a threshold to provide the necessary minimum energy to initiate the cross-linking, a further increase of pulse duration produces no additional film growth due to the lack of additional precursor. In contrast, the growth rate can even decrease at longer plasma-on times due to erosion. For a larger number of deposition cycles, the inte-

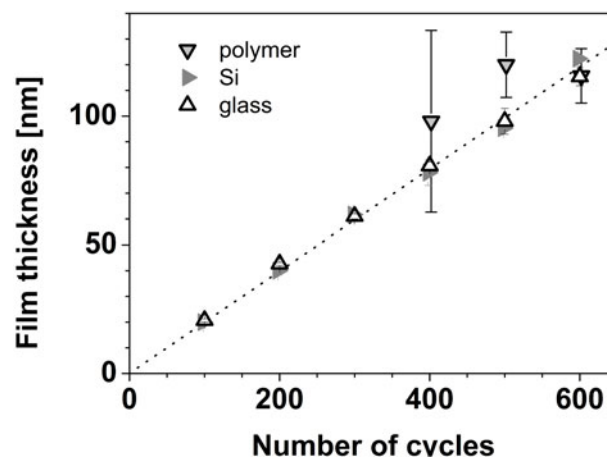


Fig. 24. Integral film thickness related to the number of deposition cycles for different substrates, according to reference [2].

gral film thickness grows linearly as shown for different substrates in Figure 24.

The deposition of thin polymer films by application of various precursors on different substrates and the prevalent experimental conditions are summarized in Table 7. The chemical composition of the deposited films has been characterized. It was found that after PE-RGD the chemical structure retention was stronger than in the case of conventional PE-CVD process.

4 Conclusion

In this paper coating methods are summarized distinguished by self-assembling or self-limiting formation processes resulting in the deposition of ultra-thin films of homogeneous thickness and partly high conformity. The presented methods are summarized in Table 8. The inclusion of plasmas can expand the process window and sometimes improve the quality of the ultra-thin films.

The development of ultra-thin films is strongly related to the transition from microelectronics to nanoelectronics. On one side the single elements become smaller and the demand for high quality dielectrics, such as high- k dielectrics, is growing, on the other side organic transistors may fulfill the demand of smaller active elements. The development of organic elements as organic light emitting diodes or organic solar cells are parts of global considerations towards effective energy consumption and renewable

Table 8. Compilation of the discussed ultra thin film deposition techniques.

Method	Self-assembling		Atomic layer deposition ALD		Molecular layer deposition MLD	
			Thermal activated	Plasma assisted	Thermal activated	Plasma Enhanced Repeated Grafting PE-RGD
Process	Spontaneous formation of well ordered molecular assemblies by adsorption of surfactant molecules on a substrate		Two sequential self-terminating chemical surface reactions			
Film type	Organic self-assembled monolayer (SAM)		Inorganic monolayer, multilayer		Organic, organic-inorganic hybrid, mono- and multilayer	Polymer, organic mono- and multilayer
Environment of film formation	Air-liquid (Langmuir-Blodgett technique)	Solution-solid vapor-solid	Vapor, atmospheric till low pressure, solid	Vapor, low pressure, solid	Vapor, low pressure, solid	Vapor, low pressure, solid
Precursor	Organic, long chain amphiphilic	Organic, surface active headgroup, functional interface group	Metal-organics, metal-halogenides		Organic, metal-organic compounds	Organic vapors
Substrates	Plane and smooth, mostly hydrophilic	Smooth, chemical bond necessary	Patterned, holes, trenches		Patterned, inorganics, polymers	Inorganics, polymers
Surface bonding	Physisorption	Chemisorption	Chemisorption		Chemisorption	
Applications	[13,19,65] Diblock nanolithography Molecular electronics Membranes Chemical/biological sensors Lubrication Optical applications (wave guides, optoelectronics)	[26,27,30,55] [108] Molecular electronics Tribology Surface wettability Anti fouling Electro-chemistry Surface passivation Corrosion resistance Protein binding Surface patterning Etch resists Biochemistry Nanostructures	[170] [182] Conformal coating of nanostructures Microelectronics High- <i>k</i> dielectric films Gate dielectrics Corrosion protection Passivation layers Diffusion barriers Low resistivity film Gas sensors Encapsulation TFT		[173] [178] [176] Conformal coating of nanostructures Flexible displays (transparent conducting films) Organic based Gas magnets separation Diffusion barriers	[2] Ultra thin polymer films with tailored surface chemistry Biomedical applications

energy technologies. The sensitivity of organic structures against environmental influences calls for an effective encapsulation. For all these tasks, ultra-thin films can provide solutions.

The authors wish to thank Prof. R. Waser (Forschungszentrum Jülich and RWTH Aachen) and Prof. K. Wandel (Sentech Instruments) for their helpful discussions and encouragement. Moreover, they thank A. Pöpke, R. Ihrke, C. Desjardins, and U. Lindemann for their assistance with the manuscript. The financial support by the German Research Foundation (DFG) in the framework of the Collaborative Research Centre Transregio 24 “Fundamentals of Complex Plasmas” is acknowledged.

References

- G. Ozaydin-Ince, A.M. Coclite, K.K. Gleason, Rep. Prog. Phys. **75**, 016501 (2012)
- A. Ohl, W. Besch, H. Steffen, R. Foest, M. Arens, K. Wandel, Plasma Process. Polym. **6**, 425 (2009)
- R. Dittmann, in *Electronic Oxides – Correlation Phenomena, Exotic Phases and Novel Functionalities*, edited by S. Blügel, Th. Brückel, R. Waser, C.M. Schneider, Lecture Notes of the 41th Spring School 2010 (Forschungszentrum Jülich, Jülich, 2010), Vol. 13
- J.A. Venables, *Introduction to surface and thin film Processes* (Cambridge University Press, 2000)
- P. Ebert, K. Szot, in *Nanoelectronics and Information Technology, Advanced Electronic Materials and Novel Devices*, edited by R. Waser, 3rd edn. (Wiley-VCH, Weinheim, 2012), pp. 255–281
- Y.B. Qi, Surf. Sci. Rep. **66**, 379 (2011)
- A. Gulino, Anal. Bioanal. Chem. **405**, 1479 (2013)
- M. Zharnikov, J. Electron Spectrosc. Relat. Phenom. **178**, 380 (2010)
- K. Ariga, J.P. Hill, M.V. Lee, A. Vinu, R. Charvret, S. Acharya, Sci. Technol. Adv. Mater. **9**, 014109 (2008)
- B. Voigtländer, S. Karthäuser, S.N. Filimonov, S.L. Tait, in *Nanoelectronics and Information Technology, Advanced Electronic Materials and Novel Devices*, edited by R. Waser, 3rd edn. (Wiley-VCH, Weinheim, 2012), pp. 305–320
- Atomic Layer Deposition of Nanostructured Materials*, edited by N. Pinna, M. Knez (Wiley-VCH Verlag, 2012)
- B. Yoon, J.L. O’Patchen, D. Seghete, A.S. Cavanagh, S.M. George, Chem. Vap. Dep. **15**, 112 (2009)
- Langmuir-Blodgett Films*, edited by G. Roberts (Plenum Press, New York, London, 1990)
- A. Ulman, *An Introduction to Ultrathin Organic Films, From Langmuir-Blodgett to Self-Assembly* (Academic Press, Boston, 1991)
- M.C. Petty, *Langmuir-Blodgett films, an introduction* (Cambridge University Press, 1996)
- G. Hähner, in *Encyclopedia of Chemical Physics and Physical Chemistry*, edited by J.H. Moore, N.D. Spencer (IOP Bristol and Philadelphia, 2001), pp. 2317–2344
- D.R. Talham, T. Yamamoto, M.W. Meiseil, J. Phys.: Condens. Matter **20**, 184006 (2008)
- S.A. Evenson, J.P.S. Badyal, C. Pearson, M.C. Petty, J. Phys. Chem. **100**, 11672 (1996)
- I.R. Peterson, J. Phys. D **23**, 379 (1990)
- S.A. Hussain, D. Bhattacharjee, Mod. Phys. Lett. B **23**, 3437 (2009)
- L. Valli, Adv. Coll. Interface Sci. **116**, 33 (2005)
- A.A. Kalachev, K. Mathauer, U. Hohne, H. Mohwald, G. Wegner, Thin Solid Films **228**, 307 (1993)
- V. Hessel, P. Detemple, J.F. Geiger, M. Keil, R. Schafer, R. Festag, J.H. Wensdorff, Thin Solid Films **286** (1996)
- E. Soterakou, K. Beltsios, T. Steriotis, N. Kanellopoulos, J. Porous Mater. **8**, 251 (2001)
- A. Ulman, Chem. Rev. **96**, 1533 (1996)
- M. Boeckl, D. Graham, Mater. Matt. **1**, 3 (2006)
- J.C. Love, L.A. Estroff, J.K. Kriebel, R.G. Nuzzo, G.M. Whitesides, Chem. Rev. **105**, 1103 (2005)
- F. Schreiber, Prog. Surf. Sci. **65**, 151 (2000)
- D.B. Mitzi, Chem. Mater. **13**, 3283 (2001)
- D.K. Aswal, S. Lenfant, D. Guerin, J.V. Yakhmi, D. Vuillaume, Anal. Chem. Acta **568**, 84 (2006)
- V.T. Joy, D. Mandler, ChemPhysChem **3**, 973 (2002)
- M. Zharnikov, A. Kuller, A. Shaporenko, E. Schmidt, W. Eck, Langmuir **19**, 4682 (2003)
- T.L. Niederhauser, Y.-Y. Lua, G. Jiang, S.D. Davis, R. Matheson, D.A. Hess, I.A. Mowat, M.R. Linfort, Angew. Chem. Int. Ed. Engl. **41**, 2353 (2002)
- H.G. Chen, X.D. Wu, Q.Q. Yu, S.R. Yang, D.P. Wang, W.Z. Shen, Chin. J. Chem. **20**, 1467 (2002)
- H.J. Himmel, M. Kaschke, P. Harder, C. Woell, Thin Solid Films **284–286**, 275 (1996)
- J.J. Benitez, S. Koptan, D.F. Ogletree, M. Salmeron, Langmuir **18**, 6096 (2002)
- S. Frey, A. Shaporenko, M. Zharnikov, P. Harder, D.L. Allara, J. Phys. Chem. B **107**, 7716 (2003)
- P.E. Laibinis, G.M. Whitesides, D.L. Allara, Y.T. Tao, A.N. Parikh, R.G. Nuzzo, J. Am. Chem. Soc. **113**, 7152 (1991)
- Z. Li, S.C. Chang, R.S. Williams, Langmuir **19**, 6744 (2003)
- F. Sinapi, L. Forget, J. Delhalle, Z. Mekhalif, Appl. Surf. Sci. **212–213**, 464 (2003)
- R. Colorado Jr., R.J. Villazana, T.R. Lee, Langmuir **14**, 6337 (1998)
- S.W. Han, S.J. Lee, K. Kim, Langmuir **17**, 6981 (2001)
- L.V. Protsailo, W.R. Fawcett, D. Russell, R.L. Meyer, Langmuir **28**, 9342 (2002)
- J.J. Hickman, P.E. Laibinis, D.I. Auerbach, C. Zou, T.J. Gardner, G.M. Whitesides, M.S. Wrighton, Langmuir **8**, 357 (1992)
- A.Y. Fadeev, R. Helmy, S. Marcinko, Langmuir **18**, 7521 (2002)
- L. Netzer, J. Sagiv, J. Am. Chem. Soc. **105**, 674 (1983)
- M. Kittelmann, P. Rahe, A. Kühnle, J. Phys.: Condens. Matter **24**, 354007 (2012)
- H.-Q. Mao, N. Li, X. Chen, Q.-K. Xue, J. Phys.: Condens. Matter **24**, 084004 (2012)
- M. Nimmrich, P. Rahe, M. Kittelmann, A. Kühnle, Phys. J. **11**, 29 (2012)
- J. Barth, Annu. Rev. Phys. Chem. **58**, 375 (2007)
- J. Repp, G. Meyer, Chimia **64**, 370 (2010)
- S.A. DiBenedetto, A. Facchetti, M.A. Ratner, T.J. Marks, Adv. Mater. **21**, 1407 (2009)
- Y.D. Park, D.H. Kim, Y. Jang, M. Hwang, J.A. Lim, K. Cho, Appl. Phys. Lett. **87**, 243509 (2005)
- H. Ma, O. Acton, G. Ting, J.W. Ka, H.L. Yip, N. Tucker, R. Schofield, A.K.-Y. Jen, Appl. Phys. Lett. **92**, 113303 (2008)

55. K. Vijayamohan, M. Aslam, Appl. Biochem. Biotechnol. **96**, 25 (2001)
56. L. Jiang, C.J. McNeil, J.M. Cooper, J. Chem. Soc. Chem. Commun., 1293 (1995)
57. K.M. Millan, S.R. Mikkelsen, Anal. Chem. **65**, 2317 (1993)
58. Y. Ishikawa, K. Okumura, T. Ishida, S. Samukawa, J. Appl. Phys. **105**, 094320 (2009)
59. S.-T. Chen, G.-S. Chen, Langmuir **27**, 12143 (2011)
60. J. Friedrich, W. Unger, A. Lippitz, Sh. Geng, I. Koprinarov, G. Kühn, St. Weidner, Surf. Coat. Technol. **98**, 1132 (1998)
61. L. Wu, E. Eisenbraun, J. Vac. Sci. Technol. B **25**, 2581 (2007)
62. Y.-T. Wu, J.-D. Liao, C.-C. Weng, M.-C. Wang, J.-E. Chang, C.-H. Chen, M. Zharnikov, Contrib. Plasma Phys. **47**, 89 (2007)
63. F.S. Bates, Science **251**, 898 (1991)
64. J.K. Cox, A. Eisenberg, R.B. Lennox, Curr. Opin. Colloid Interface Sci. **4**, 52 (1999)
65. M. Li, Ch.A. Coenjarts, Ch.K. Ober, Adv. Polym. Sci. **190**, 183 (2005)
66. P. Mansky, C.K. Harrison, P.M. Chaikin, R.A. Register, N. Yao, Appl. Phys. Lett. **68**, 2586 (1996)
67. K.L. Choy, Prog. Mater. Sci. **48**, 57 (2003)
68. R.L. Puurunen, J. Appl. Phys. **97**, 121301 (2005)
69. V. Miikkulainen, M. Leskel, M. Ritala, R.L. Puurunen, J. Appl. Phys. **113**, 021301 (2013)
70. S.M. Georges, Chem. Rev. **110**, 111 (2010)
71. P. Poodt, D.C. Cameron, E. Dickey, S.M. George, V. Kuznetsov, G.N. Parsons, F. Roozeboom, G. Sundaram, A. Vermeer, J. Vac. Sci. Technol. A **30**, 010802 (2012)
72. C.B. Musgrave, in *Atomic Layer Deposition of Nanostructured Materials*, edited by N. Pinna, M. Knez (Wiley-VCH Verlag, 2012), pp. 3–21
73. O. Sneh, R.B. Clark-Phelps, A.R. Londergan, J. Winkler, Th.E. Seidel, Thin Solid Films **402**, 248 (2002)
74. H. Kumagai, M. Matsumoto, Y. Kawamura, K. Toyoda, M. Obara, Jpn J. Appl. Phys. **33**, 7086 (1994)
75. W.J. Elam, in *Atomic Layer Deposition of Nanostructured Materials*, edited by N. Pinna, M. Knez (Wiley-VCH Verlag, 2012), pp. 227–249
76. D.D. Fong, J.A. Eastman, S.K. Kim, T.T. Fister, M.J. Highland, P.M. Baldo, P.H. Fuoss, Appl. Phys. Lett. **97**, 191904 (2010)
77. R.L. Puurunen, W. Vandervorst, J. Appl. Phys. **96**, 7686 (2004)
78. M. Putkonen, in *Atomic Layer Deposition of Nanostructured Materials*, edited by N. Pinna, M. Knez (Wiley-VCH, 2012), pp. 41–59
79. P.R. Chalker, S. Romani, P.A. Marshall, M.J. Rosseinsky, S. Rushworth, P.A. Williams, Nanotechnology **21**, 405602 (2010)
80. S.K. Kim, S. Hoffmann-Eifert, R. Waser, J. Phys. Chem. C **113**, 11329 (2009)
81. H.L. Lu, S.J. Ding, D.W. Zhang, Electrochem. Solid State Lett. **13**, G25 (2010)
82. A. Delabie, J. Rip, S. Van Elshocht, G. Pourtois, M. Mueller, B. Beckhoff, K. Pierloot, J. Vac. Sci. Technol. A **30**, 01A127 (2012)
83. K. Knapas, M. Ritala, Chem. Mater. **23**, 2766 (2011)
84. D. Seghete, G.B. Rayner Jr., A.S. Cavanagh, A.S. Cavanagh, V.R. Anderson, S.M. George, Chem. Mater. **23**, 1668 (2011)
85. M. Rooth, E. Lindahl, A. Harsta, Chem. Vap. Dep. **12**, 209 (2006)
86. R.L. Puurunen, T. Sajavaara, E. Santala, V. Miikkulainen, T. Saukkonen, M. Laitinen, M. Leskela, J. Nanosci. Nanotechnol. **11**, 8101 (2011)
87. H. Tiznado, M. Bouman, B.-C. Kang, K. Lee, F. Zaera, J. Mol. Catal. A: Chem. **281**, 35 (2008)
88. G.K. Hyde, S.D. McCullen, S. Jeon, S.M. Stewart, H. Jeon, E.G. Lobo, G.N. Parsons, Biomed. Mater. **4**, 025001 (2009)
89. B. Lee, J. Hwang, S. Lee, J. Kim, S.-M. Koo, A. Baunemann, R. Fischer, M. Sung, Angew. Chem. Int. Ed. **48**, 4536 (2009)
90. M. Knaut, M. Junige, M. Albert, J.W. Bartha, J. Vac. Sci. Technol. A **30**, 01A151 (2012)
91. A. Salaun, J. Trommer, S.B. Newcomb, I.M. Povey, M. Salaun, L. Keeney, A. O'Mahony, M.E. Pemble, Chem. Vap. Dep. **17**, 114 (2011)
92. L.D. Salmi, E. Puukilainen, M. Vehkamäki, M. Heikkilä, M. Ritala, Chem. Vap. Dep. **15**, 221 (2009)
93. Z.W. Fang, H.C. Aspinall, R. Odedra, R.J. Potter, J. Cryst. Growth **33**, 33 (2011)
94. T. Blomberg, C. Wenger, C.B. Kaynak, G. Ruhl, P. Baumann, Microelectron. Eng. **88**, 2447 (2011)
95. H.B.R. Lee, S.F. Bent, Chem. Mater. **24**, 279 (2012)
96. T.W. Scharf, S.V. Prasad, M.T. Dugger, P.G. Kotula, R.S. Goeke, R.K. Grubbs, Acta Mater. **54**, 4731 (2006)
97. R.W. Wind, F.H. Fabreguette, Z.A. Sechrist, S.M. George, J. Appl. Phys. **105**, 0974309 (2009)
98. D. Zhou, U. Schroeder, J. Xu, J. Heitmann, G. Jegert, W. Weinreich, M. Kerber, S. Knebel, E. Erben, T. Mikolajick, J. Appl. Phys. **108**, 124104 (2010)
99. D. Schmidt, E. Schubert, M. Schubert, Appl. Phys. Lett. **100**, 011912 (2012)
100. Y. Morita, S. Migita, W. Mizubayashi, H. Ota, Jpn J. Appl. Phys. **51**, 02BA04 (2012)
101. S.W. Smith, K.G. McAuliffe, J.F. Conley, Solid-State Electron. **54**, 1076 (2010)
102. I. Jogi, A. Tamm, K. Kukli, M. Kemell, J. Lu, T. Sajavaara, M. Ritala, M. Leskela, J. Electrochem. Soc. **157**, G202 (2010)
103. D.H. Levy, D. Freeman, S.F. Nelson, P.J. Cowdery-Corvan, L.M. Irving, Appl. Phys. Lett. **92**, 192101 (2008)
104. K. Hughes, J. Engstrom, J. Vac. Sci. Technol. A **28**, 1033 (2010)
105. X. Jiang, S.F. Bent, J. Phys. Chem. C **113**, 17613 (2009)
106. B.H. Lee, B. Yoon, V.R. Anderson, S.M. George, J. Phys. Chem. C **116**, 3250 (2012)
107. Y. Xu, C.B. Musgrave, Chem. Mater. **16**, 646 (2004)
108. K. Koumoto, N. Saito, Y. Gao, Y. Masuda, P. Zhu, Bull. Chem. Soc. Jpn **81**, 1337 (2008)
109. H.B.R. Lee, S.F. Bent, in *Atomic layer deposition of nanostructured materials*, edited by N. Pinna, M. Knez (Wiley-VCH, Weinheim, 2012), pp. 193–225
110. *Low Temperature Plasmas, Fundamentals, Technologies, and Techniques*, edited by R. Hippler, H. Kersten, M. Schmidt, K. Schoenbach, 2nd edn. (Wiley, 2008)
111. *Nonthermal Plasma Chemistry and Physics*, edited by J. Meichsner, M. Schmidt, R. Schneider, H.E. Wagner (CRC Press, Taylor & Francis, Boca Raton, 2013)
112. E. Kessels, H. Profijt, S. Potts, R. van de Sanden, in *Atomic Layer Deposition of Nanostructured Materials*, edited by N. Pinna, M. Knez (Wiley-VCH, 2012), pp. 131–157

113. H.B. Profijt, S.E. Potts, M.C.M. van de Sanden, W.M.M. Kessels, *J. Vac. Sci. Technol. A* **29**, 050801 (2011)
114. Y. Kim, J. Koo, J. Han, S. Choi, H. Jeon, C.-G. Park, *J. Appl. Phys.* **92**, 5443 (2002)
115. J.L. van Hemmen, S.B.S. Heil, J.H. Klootwijk, F. Roozeboom, C.J. Hodson, M.C.M. van de Sanden, W.M.M. Kessels, *J. Electrochem. Soc.* **154**, G165 (2007)
116. R.K. Grubbs, S.M. George, *J. Vac. Sci. Technol.* **24**, 486 (2006)
117. J. Joo, S.M. Rossnagel, *J. Korean Phys. Soc.* **54**, 1048 (2009)
118. S.B.S. Heil, E. Langereis, F. Roozeboom, M.C.M. van de Sanden, W.M.M. Kessels, *J. Electrochem. Soc.* **153**, G956 (2006)
119. E. Langereis, J. Keijmel, M.C.M. van de Sanden, W.M.M. Kessels, *Appl. Phys. Lett.* **92**, 23904 (2008)
120. S.E. Potts, W. Keuning, E. Langereis, G. Dingeman, M.C.M. van de Sanden, W.M.M. Kessels, *J. Electrochem. Soc.* **157**, 66 (2010)
121. L. Baker, A.S. Cavanagh, D. Seghete, S.M. George, A.J.M. Mackus, W.M.M. Kessels, Z.Y. Liu, F.T. Wagner, *J. Appl. Phys.* **109**, 08433 (2011)
122. H. Jeon, Y. Won, *Appl. Phys. Lett.* **93**, 124104 (2008)
123. Yumi Kawamura, N. Hattori, N. Miyatake, M. Horita, Y. Uraoka, *Jpn J. Appl. Phys.* **50**, 04DF05 (2011)
124. S.B.S. Heil, J.L. van Hemmen, M.C.M. van de Sanden, W.M.M. Kessels, *J. Appl. Phys.* **103**, 103302 (2008)
125. E. Langereis, H.C.M. Knoop, A.J.M. Mackus, F. Roozeboom, M.C.M. van de Sanden, W.M.M. Kessels, *J. Appl. Phys.* **102**, 083517 (2007)
126. P.K. Park, S.W. Kang, *Appl. Phys. Lett.* **89**, 192905 (2006)
127. A. Niskanen, T. Hatanpää, K. Arstila, M. Leskelä, M. Ritala, *Chem. Vap. Dep.* **13**, 408 (2007)
128. J.M. Kim, H.B.R. Lee, C. Lansalot, C. Dussarrat, J. Gatineau, H. Kim, *Jpn J. Appl. Phys.* **49**, 05FA10 (2010)
129. H.B.R. Lee, J. Kim, H. Kim, W.H. Kim, J.W. Lee, I. Hwang, *J. Korean Phys. Soc.* **56**, 104 (2010)
130. H.B.R. Lee, J.Y. Son, H. Kim, *Appl. Phys. Lett.* **90**, 213509 (2007)
131. H.B.R. Lee, H. Kim, *Electrochem. Solid State Lett.* **9**, G323 (2006)
132. A. Niskanen, A. Rahtu, T. Sajavaara, K. Arstila, M. Ritala, M. Leskela, *J. Electrochem. Soc.* **151**, G25 (2005)
133. L. Wu, E. Eisenbraun, *Electrochem. Solid State Lett.* **11**, H107 (2008)
134. S.W. Kim, S.H. Kwon, S.J. Jeong, J.S. Park, S.W. Kang, *Electrochem. Solid State Lett.* **11**, H303 (2008)
135. H.B.R. Lee, S.H. Bang, W.H. Kim, G.H. Gu, Y.K. Lee, T.M. Chung, C.G. Kim, C.G. Park, H. Kim, *Jpn J. Appl. Phys.* **49**, 05FA11 (2010)
136. G.A. Ten Eyck, S. Pimangang, J.S. Juneja, H. Bakhru, T.M. Lu, G.C. Wang, *Chem. Vap. Dep.* **13**, 307 (2007)
137. N.E. Lay, G.A.T. Eyck, D.J. Duquette, T.M. Lu, *Electrochem. Solid State Lett.* **10**, D13 (2007)
138. H. Wojcik, U. Merkel, A. Jahn, K. Richter, M. Junige, C. Klein, J. Gluch, M. Albert, F. Munnik, C. Wenzel, J.W. Bartha, *Microelectron. Eng.* **88**, 641 (2011)
139. N. Leick, R.O.F. Verkuijlen, L. Lamagna, E. Langereis, S. Rushworth, F. Roozeboom, M.C.M. van de Sanden, W.M.M. Kessels, *J. Vac. Sci. Technol. A* **29**, 021016 (2011)
140. W. Sari, T.K. Eom, S.H. Kim, H. Kim, *J. Electrochem. Soc.* **158**, D42 (2011)
141. H. Kim, S.M. Rossnagel, *Thin Solid Films* **441**, 311 (2003)
142. H. Kim, C. Cabral, C. Lavoie, S.M. Rossnagel, *J. Vac. Sci. Technol.* **20**, 1321 (2002)
143. S.M. Rossnagel, A. Sherman, F. Turner, *J. Vac. Sci. Technol. B* **18**, 2016 (2000)
144. H. Kim, S.M. Rossnagel, *J. Vac. Sci. Technol.* **20**, 802 (2002)
145. S.E. Potts, L. Schmalz, M. Fenker, B. Diaz, J. Swiatowska, V. Maurice, A. Seyeux, P. Marcus, G. Radnoczi, L. Toth, W.M.M. Kessels, *J. Electrochem. Soc.* **158**, C132 (2011)
146. W.S. Kim, D.Y. Moon, B.W. Kang, J.W. Park, J.G. Park, *J. Korean Phys. Soc.* **55**, 55 (2009)
147. R. Lossy, H. Gargouri, M. Arens, J. Würfl, *J. Vac. Sci. Technol. A* **31**, 01A140 (2013)
148. G.X. Liu, F.K. Shan, W.J. Lee, B.C. Shin, S.C. Kim, H.S. Kim, C.R. Cho, *Integr. Ferroelectr.* **94**, 11 (2007)
149. N.J. Seong, E.T. Kim, S.G. Yoon, *Integr. Ferroelectr.* **74**, 181 (2005)
150. A. Delabie, M. Caymax, S. Gielis, J.W. Maes, L. Nyns, M. Popovici, J. Swerts, H. Tielens, J. Peeters, S. Van Elshocht, *Electrochem. Solid State Lett.* **13**, H176 (2010)
151. W.J. Maeng, G.H. Gu, C.G. Park, K. Lee, T. Lee, H. Kim, *J. Electrochem. Soc.* **156**, G109 (2009)
152. S.B.S. Heil, J.L. van Hemmen, C.J. Hodson, N. Singh, J.H. Klootwijk, F. Roozeboom, M.C.M. van de Sanden, W.M.M. Kesseles, *J. Vac. Sci. Technol. A* **25**, 1357 (2007)
153. P.K. Park, J.S. Roh, B.H. Choi, S.W. Kang, *Electrochem. Solid State Lett.* **9**, F34 (2006)
154. W.H. Kim, W.J. Maeng, K.J. Moon, J.M. Myong, H. Kim, *Thin Solid Films* **519**, 362 (2010)
155. B.Y. Kim, M.G. Ko, E.J. Lee, M.S. Hong, Y.J. Jeon, J.W. Park, *J. Korean Phys. Soc.* **49**, 1303 (2006)
156. S.J. Won, S. Suh, M.S. Huh, H.J. Kim, *IEEE Electron. Device Lett.* **31**, 857 (2010)
157. J.W. Lim, S.J. Yun, J.H. Lee, *ETRI J.* **27**, 118 (2005)
158. D.H. Kim, S.W. Kim, S.B. Lee, S.H. Hong, *Sens. Actuat. B Chem.* **147**, 653 (2010)
159. W.J. Maeng, J.W. Lee, J.M. Myong, H. Kim, *Jpn J. Appl. Phys.* **46**, 3224 (2007)
160. N.G. Kubala, C.A. Wolden, *Thin Solid Films* **518**, 6733 (2010)
161. C.S. Lee, J. Kim, G.H. Gu, D.H. Jo, C.G. Park, W. Choi, H. Kim, *Thin Solid Films* **518**, 4757 (2010)
162. S. Kim, S.L. Brown, S.M. Rossnagel, J. Bruley, M. Copel, M.J.P. Hopstaken, V. Narayanan, M.M. Frank, *J. Appl. Phys.* **107**, 054102 (2010)
163. W.J. Jeon, H.S. Chung, D. Joo, S.W. Kang, *Electrochem. Solid State Lett.* **11**, H19 (2008)
164. J. Musschoot, D. Deduytsche, H. Poelman, J. Haemers, R.L. Van Meirhaeghe, S. Van den Berghe, C. Detavernier, *J. Electrochem. Soc.* **156**, P122 (2009)
165. S.K. Kwon, D.W. Kim, Y.H. Jung, B.J. Lee, *J. Korean Phys. Soc.* **55**, 999 (2009)
166. D.L. Zhao, D.A. Mourey, T.N. Jackson, *IEEE Electron. Device Lett.* **31**, 323 (2010)
167. S.E. Potts, C.J. Carmalt, C.S. Blackman, F. Abou-Chahine, N. Leick, W.M.M. Kessels, H.O. Davies, P.N. Heys, *Inorg. Chim. Acta* **363**, 1077 (2010)
168. Y. Tak, K. Yong, *Surf. Rev. Lett.* **12**, 215 (2005)

169. S.J. Yun, J.W. Lim, J.H. Lee, *Electrochem. Solid State Lett.* **7**, F81 (2004)
170. S.J. Yun, J.B. Koo, J.W. Lim, S.H. Kim, *Electrochem. Solid State Lett.* **10**, H90 (2007)
171. S.M. George, B. Yoon, A.A. Dameron, *Acc. Chem. Res.* **42**, 498 (2009)
172. S.M. George, B. Yoon, R.A. Hall, A.I. Abdulagatov, Z.M. Gibbs, Y. Lee, D. Seghete, B.H. Lee, in *Atomic Layer Deposition of Nanostructured Materials*, edited by N. Pinna, M. Knez (Wiley-VCH, 2012), pp. 83–107
173. S.M. George, *The Strem Chemiker* **25**, 13 (2011)
174. Y. Du, S.M. George, *J. Phys. Chem. C* **111**, 8509 (2007)
175. A.A. Dameron, D. Seghete, B.B. Burton, S.D. Davidson, A.S. Cavanagh, J.A. Bertrand, S.M. George, *Chem. Mater.* **20**, 3315 (2008)
176. C.-Y. Kao, J.-W. Yoo, Y. Min, A.J. Epstein, *ACS Appl. Mater. Interfaces* **4**, 137 (2012)
177. K.-S. Yoon, K.-S. Han, M.-M. Sung, *Nano. Res. Lett.* **7**, 71 (2012)
178. B. Gong, Q. Peng, G.N. Parsons, *J. Phys. Chem. B* **115**, 5930 (2011)
179. T. Yoshimura, S. Tatsuura, W. Sotoyama, *Appl. Phys. Lett.* **59**, 482 (1991)
180. T. Yoshimura, S. Tatsuura, W. Sotoyama, A. Metsuura, T. Hayano, *Appl. Phys. Lett.* **60**, 268 (1992)
181. N.M. Adarnczyk, A.A. Dameron, S.M. George, *Langmuir* **24**, 2081 (2008)
182. W.J. Potscavage, S. Yoo, B. Domercq, B. Kippelen, *Appl. Phys. Lett.* **90**, 253511 (2007)